

An Improved Chimp Optimization Algorithm for Short-term Hydrothermal Scheduling

Gonggui Chen, Shumin Wang, Yongsheng He, Wanfeng Shang, Hongyu Long

Abstract— The short-term hydrothermal scheduling (STHS) is a complex non-linear, non-convex and high-dimensional mathematical optimization problem. Due to the fact that the original chimp optimization algorithm (ChOA) is likely to fall into local optimum and has the disadvantage of low population diversity, an improved chimp optimization algorithm (IChOA) is proposed to solve the STHS problem. Firstly, Logistic-Tent chaotic mapping is employed to initialize the population and increase the population diversity. Then a new nonlinear convergence factor is introduced to make the optimization search process more applicable to STHS problems. Next, particle swarm algorithm (PSO) and gravitational search algorithm (GSA) are combined to enhance the shortcoming and balance the global search ability and local exploration ability of ChOA. Moreover, Cauchy mutation and opposition-based learning strategy are supplemented as perturbation interference when the optimal position is not updated to improve the ability to leap out of the local optimum. Finally, a graded optimization strategy is adopted for the constraint handling of dynamic reservoir balance and thermal power balance. Three standard hydrothermal power systems are utilized to verify the practicability and validity of the proposed method. Results of simulations reveal that IChOA has significant competitive advantages in addressing the STHS problem.

Index Terms— short-term hydrothermal scheduling (STHS), Logistic-Tent map, Cauchy mutation, opposition-based learning strategy, graded optimization strategy.

I. INTRODUCTION

In recent years, the rise of the national economic level and the expansion of the power system have attracted extensive attention, and the issue of energy consumption in social production and life cannot be ignored. The short-term hydrothermal scheduling (STHS) is one of the effective technical means to ensure the safe, stable and economic

operation of the power system, whose task is to obtain the optimal scheduling scheme with the lowest fuel cost while meeting the given constraints of the power system [1]. Hydropower is a pollution-free and sustainable energy source, so the cost of STHS is mainly generated by thermal plants. The STHS problem is essentially a multivariate, high-dimensional, real-time dynamic non-linear and non-convex mathematical optimization problem with complex constraint limitations [2, 3]. Due to the intricate structure between cascade hydropower plants, the valve point effect of thermal plants and the transmission loss in the power system, the nonlinearity, non-smoothness and non-convex characteristics of the STHS problem are more prominent and more difficult to solve.

At present, researchers have proposed numerous solutions to solve the STHS problem, which can be divided into two categories: traditional classical optimization algorithms and artificial intelligence optimization algorithms. Conventional algorithms include linear programming (LP) [4], nonlinear programming (NLP) [5], dynamic programming (DP) [6], mixed integer programming (MIP) [7], Lagrange relaxation (LR) [8], gradient search techniques (GS) [9] and Newton's method [10]. The LP is only applicable to the study of extreme value problems with linear objective functions under linear constraints, and using approximate linearization to deal with nonlinear problems will reduce the solution accuracy. The NLP is long in computation time, slow in convergence, and it requires the objective function to be continuously differentiable. When dealing with large-scale optimization problems, the DP is highly prone to dimensional disaster, which may lead to dire consequences that are difficult to control. And the MIP will exhibit the drawback of low computational efficiency. The LR method is more effective in dealing with large-scale problems, but the pairwise gap oscillation may occur during convergence, making the problem diverge. The GS is applicable to segmented linear objective functions and impractical to be applied to the SHTS problem. The Newton's method is one of the most promising ways to solve nonlinear optimization problems, but the repeated computation of Jacobi matrices increases the computational complexity and is no longer as applicable for large-scale problems.

On the contrary, modern meta-heuristic intelligent optimization algorithms that has robust structure and strong robustness are less restrictive for solving the STHS problem and do not require continuous differentiability of the objective function, which are more adaptable and systematic, such as genetic algorithm (GA) [11], differential evolution (DE) [12], particle swarm optimization (PSO) [13], Hopfield neural network (HNN) [14], artificial bee colony algorithm (ABC) [15] and grasshopper optimization algorithm (GOA) [16], etc. Nonetheless, there still exist some shortcomings in the basic artificial optimization algorithms, such as slow convergence speed, poor global

Manuscript received January 10, 2022; revised May 13, 2022. This work was supported by the National Natural Science Foundation of China (51207064).

Gonggui Chen is a professor of Key Laboratory of Industrial Internet of Things and Networked Control, Ministry of Education, Chongqing University of Posts and Telecommunications, Chongqing 400065, China; Chongqing Key Laboratory of Complex Systems and Bionic Control, Chongqing University of Posts and Telecommunications, Chongqing 400065, China (e-mail: chenggpw@126.com).

Shumin Wang is a graduate student of Chongqing University of Posts and Telecommunications, Chongqing 400065, China (e-mail: shuminwang229@163.com).

Yongsheng He is a senior engineer of State Grid Chongqing Electric Power Company, Chongqing, China, Chongqing 400015, China (e-mail: 120204302@qq.com).

Wanfeng Shang is an associate professor of Guangdong Provincial Key Lab of Robotics and Intelligent System, Shenzhen Institute of Advanced Technology, Chinese Academy of Sciences Shenzhen, Shenzhen 518055, China (e-mail: wf.shang@siat.ac.cn).

Hongyu Long is a professor level senior engineer of Chongqing Key Laboratory of Complex Systems and Bionic Control, Chongqing University of Posts and Telecommunications, Chongqing 400065, China (corresponding author to provide phone: +8613996108500; e-mail: longhongyu20@163.com).

search capability or weak local search capability, etc. Consequently, researchers have proposed a variety of improvement strategies for the defects of different algorithms and successfully applied them to the STHS problem. For instance, modified chaotic differential evolution (MCDE) [17], optimal gamma based genetic algorithm (OGB-GA) [18], modified cuckoo search algorithm (MCSA) [19], modified social group optimization (MSGO) [20], accelerated particle swarm optimization (APSO) [21] and a hybrid of real coded genetic algorithm and artificial fish swarm algorithm (RCGA-AFSA) [22], etc. And the effectiveness of these improved algorithms has been verified through specific simulation experiments. Meanwhile, the superiority of the performance of the new nature-inspired artificial intelligence algorithms in dealing with multi-dimensional and multi-module mathematical optimization problems is also demonstrated.

Chimp optimization algorithm (ChOA) [23] is a novel metaheuristic optimization algorithm proposed by Khishe and Mosavi et al. based on chimp group hunting behavior in 2020. Compared with other swarm intelligence algorithms, ChOA not only has fewer parameters to be regulated, but also is easy to understand and implement. Despite all this, there is still much room for improvement in its convergence speed and optimization accuracy. The improvement ideas can take example by some improvement strategies of similar algorithms as whale optimization algorithm (WOA) [24] and gray wolf optimizer (GWO) [25]. For example, an improved whale optimization algorithm based on nonlinear adaptive weight and golden sine operator (NGS-WOA) [26] has been proposed aiming at the shortcomings of WOA such as low precision and slow convergence speed. In addition, an improved grey wolf optimizer based on tracking mode (TGWO) and seeking mode (SGWO) [27] has been proposed to improve the diversity of the population and the ability of the algorithm to balance exploration and exploitation. This paper proposes an improved chimp optimization algorithm (IChOA) to solve the STHS problem: firstly, initialize chimp individuals using Logistic-Tent chaotic mapping to make the population individuals as uniformly distributed as possible; secondly, come up with a nonlinear convergence factor update strategy to balance the global search and local search capabilities of the algorithm; thirdly, combine the particle swarm optimization (PSO) [28] and gravitational search algorithm (GSA) [29, 30] speed update formulation to improve the global search ability of ChOA; last, integrate Cauchy mutation and opposition-based learning strategy and carry out disturbance mutation when the optimal position remains unchanged.

The remaining chapters of this article are arranged as follows. The mathematical formulation of STHS including constraints is presented in section II. Section III makes a detailed overview of the ChOA and its improvement strategies. Section IV introduces the constraints handling methods and the applications of IChOA for the STHS problem. Section V presents the simulation results and discussion. The last section summarizes the former parts and makes an outlook analysis.

II. THE PROBLEM FORMULATION

A. The Objective Function

The main goal of STHS is to find the optimal scheduling solution and minimize the total operation cost of the power

system on the premise of meeting the power system constraints. The objective function of the STHS problem is expressed as minimum fuel cost, and its formula is as follows:

$$\min F_C = \sum_{t=1}^T \sum_{i=1}^{N_s} F_{C_{it}}(P_{it}^{tp}) \quad (1)$$

where F_C represents the total fuel cost in the whole scheduling cycle, T represents the total hours, N_s is the total number of thermal plants, P_{it}^{tp} shows the power output of i th thermal plant at t hour, $F_{C_{it}}(P_{it}^{tp})$ shows the fuel expense of i th thermal plant at t hour. The fuel cost ignoring the valve point effect is represented by the following quadratic function:

$$F_{C_{it}}(P_{it}^{tp}) = a_i (P_{it}^{tp})^2 + b_i P_{it}^{tp} + c_i \quad (2)$$

Ignoring the valve point effect can not fully reflect the real situation. The power system operation cost function considering valve point effect is composed of the superposition of smooth quadratic function and sinusoidal function, showing nonlinear characteristics, which is expressed as follows:

$$F_{C_{it}}(P_{it}^{tp}) = a_i (P_{it}^{tp})^2 + b_i P_{it}^{tp} + c_i + |d_i \sin(e_i (P_{i,\min}^{tp} - P_{it}^{tp}))| \quad (3)$$

where a_i , b_i , c_i , d_i , e_i are cost the coefficients of the i th generator unit, an $P_{i,\min}^{tp}$ corresponds to the minimum output power of thermal plant i .

B. The Constraints

The above objective functions are all subject to system constraints include equality constraints and inequality constraints, which are indispensable to ensure the normal operation of the STHS system.

1) The equality constraints

Considering the transmission loss of power system, the power system must maintain a dynamic balance among the total output power, transmission loss and real load demand.

$$\sum_{i=1}^{N_s} P_{it}^{tp} + \sum_{j=1}^{N_h} P_{jt}^{hp} = P_{Dt} + P_{Lt} \quad (4)$$

where N_h is the total amount of hydropower plants, P_{it}^{hp} represents the output power of i th hydropower plant at t hour, P_{Dt} represents the total actual load demand of the power system in period t and P_{Lt} represents the total transmission loss during time interval t .

The power generation capacity of a hydropower plant is determined by both the discharge volume and the reservoir capacity value of the hydropower plant, which is calculated as follows:

$$P_j^{hp} = C_{j1} (V_{jt}^{hp})^2 + C_{j2} (Q_{jt}^{hp})^2 + C_{j3} V_{jt}^{hp} Q_{jt}^{hp} + C_{j4} V_{jt}^{hp} + C_{j5} Q_{jt}^{hp} + C_{j6} \quad (5)$$

where V_{jt}^{hp} is the reservoir capacity of hydropower plant j at t hour, Q_{jt}^{hp} is the discharge volume of hydropower plant j at t hour, and C_{j1} , C_{j2} , C_{j3} , C_{j4} , C_{j5} , C_{j6} are the constant coefficients of hydropower plant j .

The reservoir capacity value of the hydropower plant is constantly changing at each time, which is expressed by the following equation:

$$V_{jt}^{hp} = V_{j(t-1)}^{hp} + I_{jt}^{hp} - Q_{jt}^{hp} - S_{jt}^{hp} + \sum_{m=1}^{R_j} (Q_{m(t-\tau_m)}^{hp} - S_{m(t-\tau_m)}^{hp}) \quad (6)$$

where I_{jt}^{hp} and S_{jt}^{hp} are the inflow and spillage of hydropower plant j at t hour respectively, τ_m indicates the drainage delay time between cascade hydropower stations. R_j stands for the number of connected reservoirs between the current reservoir and the upper reservoir. The water spillage is not considered and is made to zero in this paper.

The transmission loss of power system P_{L_t} can be calculated by the Krons formula [31], where B_{ij} , B_{i0} and B_{00} represent the transmission loss coefficients, N is the total number of thermal plants and hydropower plants.

$$P_{L_t} = \sum_{i=1}^N \sum_{j=1}^N P_{it}^{tp} B_{ij} P_{jt}^{hp} + \sum_{i=1}^N B_{i0} P_{it}^{tp} + B_{00} \quad (7)$$

There is a special restriction that needs to be strictly enforced, that is, the storage capacity values of all reservoirs at the start and end of the dispatch must strictly comply with the initial and final reservoir volume.

$$V_{j0}^{hp} = V_{j,initial}^{hp}, V_{jT}^{hp} = V_{j,final}^{hp} \quad (8)$$

where $V_{j,initial}^{hp}$ and $V_{j,final}^{hp}$ are the initial and final reservoir volume of hydropower plant j respectively.

2) The inequality constraints

The output power of each thermal plant and hydropower plant cannot be less than the minimum output power and cannot exceed the maximum output power.

$$P_{i,min}^{tp} \leq P_{it}^{tp} \leq P_{i,max}^{tp} \quad i = 1, 2, \dots, N_s, t = 1, 2, \dots, T \quad (9)$$

$$P_{j,min}^{hp} \leq P_{jt}^{hp} \leq P_{j,max}^{hp} \quad j = 1, 2, \dots, N_h, t = 1, 2, \dots, T \quad (10)$$

where $P_{i,min}^{tp}$ and $P_{i,max}^{tp}$ are the minimum and maximum power output of thermal plant i respectively, $P_{j,min}^{hp}$ and $P_{j,max}^{hp}$ are the minimum and maximum power output of hydropower plant j respectively.

The real-time reservoir capacity of each reservoir must be within the given range, and it is not allowed to be lower than $V_{j,min}^{hp}$ or higher than $V_{j,max}^{hp}$.

$$V_{j,min}^{hp} \leq V_{jt}^{hp} \leq V_{j,max}^{hp} \quad j = 1, 2, \dots, N_h, t = 1, 2, \dots, T \quad (11)$$

Similarly, the discharge volume of hydropower plants should also be limited between the maximum discharge volume $Q_{j,max}^{hp}$ and minimum discharge volume $Q_{j,min}^{hp}$.

$$Q_{j,min}^{hp} \leq Q_{jt}^{hp} \leq Q_{j,max}^{hp} \quad j = 1, 2, \dots, N_h, t = 1, 2, \dots, T \quad (12)$$

III. THE OVERVIEW OF CHOA AND ITS IMPROVEMENT

A. Chimp Optimization Algorithm

ChOA is inspired by the group hunting behavior of chimps, which achieve the purpose of solving problems by simulating the cooperative hunting behavior of four types of chimps: the attacker, the barrier, the chaser and the driver. Different roles undertake different tasks in the procedure of hunting. According to reference[23], the mathematical model of ChOA is as follows.

1) Driving and Chasing the Prey

During hunting process, each individual chimp can change its position in the space around the prey randomly, which is mathematically described as follows.

$$D = |C \cdot X_{prey}(t) - m \cdot X_{chimp}(t)| \quad (13)$$

$$X_{chimp}(t+1) = X_{chimp}(t) - A \cdot D \quad (14)$$

where t denotes the current iteration, X_{prey} stands for the vector of prey position and X_{chimp} represents the position vector of a chimp, A , m and C are the coefficients vectors

that are calculated by Eq.(15), (16) and (17), respectively.

$$A = 2f \cdot r_1 - f \quad (15)$$

$$m = \text{Chaotic_value} \quad (16)$$

$$C = 2r_2 \quad (17)$$

where r_1 and r_2 are random vectors in the range of $[0, 1]$, f is the convergence factor, whose value decreases linearly from 2 to 0 as the number of iterations increases, m is the chaotic mapping vector, which represents the influence of the sexual motivation of chimps in the hunting process.

A is a random vector that determines the distance between chimpanzees and prey, whose value is a random number between $[-f, f]$. When $|A| \leq 1$, it indicates that the chimp individual tends to the prey position; when $|A| > 1$, it indicates that the chimp individual deviates from the prey position and searches for prey in a broader range.

C is the control coefficient for the chimp to drive and chase prey, who is a random number between $[0, 2]$. When $C < 1$, it means that the influence of the prey position on the chimp position is weakened, and vice versa.

2) Attacking Mode

Suppose that the initial population of chimps is NP , then the position of the i th chimp is X_i . After initializing the population, the optimal solution $X_{Attacker}$, the second optimal solution $X_{Barrier}$, the third optimal solution X_{Chaser} and the fourth optimal solution X_{Driver} are determined. The positions of other chimps are renewed according to the positions of the four chimps, which are described by Eq.(18)-(20) below.

$$\begin{cases} D_{Attacker} = |C_1 \cdot X_{Attacker} - m_1 \cdot X| \\ D_{Barrier} = |C_2 \cdot X_{Barrier} - m_2 \cdot X| \\ D_{Chaser} = |C_3 \cdot X_{Chaser} - m_3 \cdot X| \\ D_{Driver} = |C_4 \cdot X_{Driver} - m_4 \cdot X| \end{cases} \quad (18)$$

$$\begin{cases} X_1 = X_{Attacker} - A_1 \cdot D_{Attacker} \\ X_2 = X_{Barrier} - A_2 \cdot D_{Barrier} \\ X_3 = X_{Chaser} - A_3 \cdot D_{Chaser} \\ X_4 = X_{Driver} - A_4 \cdot D_{Driver} \end{cases} \quad (19)$$

$$X(t+1) = \frac{X_1 + X_2 + X_3 + X_4}{4} \quad (20)$$

where X refers to the position vector of the current chimp, $X(t+1)$ refers to the updated position vector of the current chimp.

3) Attacking and Searching for the Prey

In the final stage of hunting process, on the one hand, chimps revise their positions depending upon the positions of the attacker, the barrier, the chaser and the driver and attack the prey; on the other hand, chimps demonstrate the exploration process through dispersing in search of the prey.

4) Social Incentive

After acquiring food satisfaction, social motivation causes individual chimps to relinquish their hunting duties and attempt to obtain food forcibly and disorderly. The chaotic behavior in final stage contributes ChOA to surmount the drawbacks of falling into local optimization and slow convergence when solving high-dimensional problems.

$$X_{chimp}(t+1) = \begin{cases} X_{prey}(t) - A \cdot D & (\mu \leq 0.5) \\ \text{Chaotic_value} & (\mu > 0.5) \end{cases} \quad (21)$$

where μ is a stochastic number between $[0, 1]$.

B. Improved Chimp Optimization Algorithm

Despite the fact that ChOA outperforms the similar algorithms WOA and GWO in terms of algorithm performance, there are still some drawbacks. Aiming at improving the fundamental defects of the basic ChOA, such as relying on the initial population, easily falling into local optimum and slow convergence speed, this paper introduces the following corresponding strategies.

1) Logistic-Tent Chaotic initialization

While ChOA is used to address STHS problem, the rand function is adopted to initialize the population randomly, which results in a low population traversal and uneven distribution in the solution space. Thus it will affect the search efficiency and solution accuracy of the algorithm. In this paper, Logistic-Tent chaotic mapping is introduced to initialize the population, so as to improve the population diversity, make the initial chimp individuals more uniformly distributed throughout the whole solution space and discover the position of the superior solution more quickly. Therefore, the convergence speed of the algorithm is accelerated and the accuracy of the algorithm in finding the superiority is enhanced. The mathematical formulation of Logistic-tent chaotic mapping is expressed as follows.

$$m_{n+1} = \begin{cases} \left[rm_n(1-m_n) + \frac{(4-r)}{2} m_n \right] \bmod 1 & (m_n < 0.5) \\ \left[rm_n(1-m_n) + \frac{(4-r)(1-m_n)}{2} \right] \bmod 1 & (m_n \geq 0.5) \end{cases} \quad (22)$$

where r is introduced to control the proportion of Logistic mapping and Tent mapping. The initial value m_0 is generated at random between $[0, 1]$, and then update m according to Eq.(22).

2) Nonlinear factor update strategy

Global search capability and local exploitation capability are two basic attributes to measure the performance of heuristic intelligence algorithms, and how to balance these two attributes is the crucial to algorithm performance improvement. From the description of the ChOA in the previous chapter, it is evident that when $|A| > 1$, chimp individuals search for prey in a scattered manner, corresponding to the global search; when $|A| \leq 1$, chimp individuals tend to prey, corresponding to the local search. According to Eq.(15), the value of A depends on the convergence factor f . The convergence factor f of the original ChOA decreases linearly from 2 to 0 as the iteration number increasing, and this linear change cannot be adapted to the optimization-seeking process of ChOA for the STHS problem, which will lead to slow convergence and fall into local optimum prematurely.

In order to balance the global search and local search capabilities of ChOA and make it more practically applicable to the STHS problem, this paper proposes a nonlinear convergence factor update strategy with the mathematical expression shown below.

$$f = f_{\text{initial}} \cdot \left[1 - \left(\frac{e^{\ln t / \ln t_{\max}} - 1}{e - 1} \right) \right]^\lambda \quad (23)$$

where f_{initial} is the initial value of the convergence factor, t is the current iteration number, t_{\max} is the maximum iteration number, and λ is the nonlinear adjustment factor.

3) Position update adjustment strategy

The basic ChOA follows the leaders of four types of chimp individuals when performing position updating, namely the attacker, the barrier, the chaser and the driver. However, this update mechanism does not take each individual chimp's own search experience into account, resulting in the algorithm easily falling into local optimality and low search accuracy. The search mechanism of PSO and GSA are combined in a certain way, which can compensate for the principle deficiencies of ChOA and enhance the exploration and exploitation capabilities of the algorithm.

a) Particle Swarm Optimization (PSO)

PSO [28] is an artificial intelligence algorithm that simulates birds predation proposed by Kennedy and Eberhart in 1995, whose basic concept is to search for the optimal solution through collaboration and information sharing among individuals in the population. Anyone of particles can adjust its own direction of movement according to its own experience and memory, learn and remember the information from other particles in the group. In short, all the particles in the swarm continuously adjust their velocity and position according to their historical optimal position and the global optimal position shared by the whole swarm. The velocity update equation of the particles is as follows.

$$v_{Pi}^d(t+1) = \omega v_{Pi}^d(t) + c_1 r_1 (P_{i,best}^d - X_i) + c_2 r_2 (G_{i,best}^d - X_i) \quad (24)$$

where ω is the inertia factor; $P_{i,best}^d$ is the historical optimal position of the i th particle; $G_{i,best}^d$ is the current global optimal position of the particle swarm; c_1 and c_2 represent the learning factor constants; r_1 and r_2 are random numbers transformed in the range $[0,1]$.

b) Gravitational Search Algorithm (GSA)

GSA [29] is a meta-heuristic intelligent optimization algorithm based on Newton's law of universal gravitation proposed by Rashdei et al. in 2009, which mainly uses the law of gravity between two objects to guide the motion optimization of each particle and search for the optimal solution, with outstanding global optimization capability. The gravitational force between two particles is proportional to the mass of the two particles and inversely proportional to the distance between the two particles. The gravitational force between the particles and the related parameters are calculated as follows.

$$F_{ij}^d(t) = G(t) \frac{M_i(t) \times M_j(t)}{R_{ij} + \varepsilon} (X_j^d(t) - X_i^d(t)) \quad (25)$$

$$F_i^d(t) = \sum_{j=1, j \neq i}^N r_3 F_{ij}^d(t) \quad (26)$$

where $F_{ij}^d(t)$ is the gravitational force between particle i and j ; $M_i(t)$ and $M_j(t)$ are the masses of particle i and j respectively; R_{ij} is the Euclidean distance; ε is a constant close to 0; $F_i^d(t)$ is the weighted sum of the gravitational effect of i by other particles; r_3 is a random number between $[0, 1]$.

The gravitational constant $G(t)$ and the mass of the particle $M_i(t)$ are calculated by the following equation.

$$G(t) = G_0 e^{-\frac{t}{t_{\max}}} \quad (27)$$

$$M_i(t) = \frac{m_i(t)}{\sum_{j=1}^N m_j(t)} \quad (28)$$

$$m_i(t) = \frac{Fit_i(t) - F_{worst}(t)}{F_{best}(t) - F_{worst}(t)} \quad (29)$$

$$a_i^d(t) = \frac{F_i^d(t)}{M_i(t)} \quad (30)$$

where a is a constant, $Fit_i(t)$ is the fitness function value of particle i in the t generation, $F_{best}(t)$ and $F_{worst}(t)$ represent the best value and the worst value of the fitness in the t generation respectively. $a_i^d(t)$ denotes the acceleration.

The speed update formula of GSA is shown below. r_4 is a random number between $[0, 1]$.

$$v_{Gi}^d(t+1) = r_4 v_{Gi}^d(t) + a_i^d(t) \quad (31)$$

c) Position update mechanism

This paper proposes a new position update mechanism. The individual memory function of PSO is introduced into the position update formulation of ChOA. At the same time, using the characteristic that GSA is not affected by historical and global optimal particle, the global search ability and local development ability of the algorithm are effectively balanced. The new position update method is shown below.

$$X(t+1) = \frac{X_1 + X_2 + X_3 + X_4}{4} + b_1 v_{pi}^d(t+1) + b_2 v_{Gi}^d(t+1) \quad (32)$$

where b_1 and b_2 are random numbers between $[0,1]$, and satisfy $b_1+b_2=1$.

4) Cauchy mutation and Opposition-based learning

When ChOA falls into the local optimum and the optimal solution is not updated. Cauchy mutation and Opposition-based learning strategies are introduced on the basis of the above improvement methods. When the specified number of iterations has been reached and the optimal solution has not been updated, the target position is perturbed and updated according to the probability to make the algorithm jump out of the local optimum and further enhance the global search capability of the algorithm.

Opposition-based learning [32] is a new computational intelligence technique proposed by Tizhoosh in 2005, which aims to find the corresponding reverse solution based on the current optimal solution, and select and preserve the better solution by evaluation. The mathematical representation of incorporating Opposition-based learning into ChOA is as follows.

$$X_{best}^*(t) = ub + r \oplus (lb - X_{best}(t)) \quad (33)$$

$$X_{best}(t+1) = X_{best}^*(t) + b_1 \oplus (X_{best}(t) - X_{best}^*(t))$$

where $X_{best}^*(t)$ is the inverse of the optimal solution, ub and lb are the upper and lower bounds respectively, r is the random number matrix and b_1 is the information exchange coefficient [33], which is expressed as follows.

$$b_1 = \left(1 - \frac{t}{t_{max}}\right)^t \quad (34)$$

The Cauchy operator is inserted into the position update formula of ChOA to exploit the perturbation ability of the Cauchy operator and strengthen the ability of the algorithm

to jump out of the local optimum.

$$X_{best}(t+1) = X_{best}(t) + Cauchy(0,1) \oplus X_{best}(t) \quad (35)$$

where $Cauchy(0,1)$ is the standard Cauchy distribution.

Then whether to use Opposition-based learning strategy or Cauchy mutation method is determined by the selection probability P_s [33], which is expressed as follows.

$$P_s = -\exp\left(1 - \frac{t}{t_{max}}\right)^{20} + \theta \quad (36)$$

where θ is the adjustment factor whose value is taken as 0.05.

If $P_s > rand$, choose Opposition-based learning strategy to update position, otherwise choose Cauchy mutation to update position.

Although the above two perturbation strategies enhance the ability of the algorithm to leap out of the local space, it cannot guarantee that the new position after the perturbation variation is better than the original position, so a greedy mechanism is added after the perturbation update to retain the optimal target position.

$$X_{best} = \begin{cases} X_{new}, & F(X_{new}) \leq F(X_{best}) \\ X_{best}, & F(X_{new}) > F(X_{best}) \end{cases} \quad (37)$$

The flow chart of the IChOA combined with the above improvement measures is shown in Fig. 1.

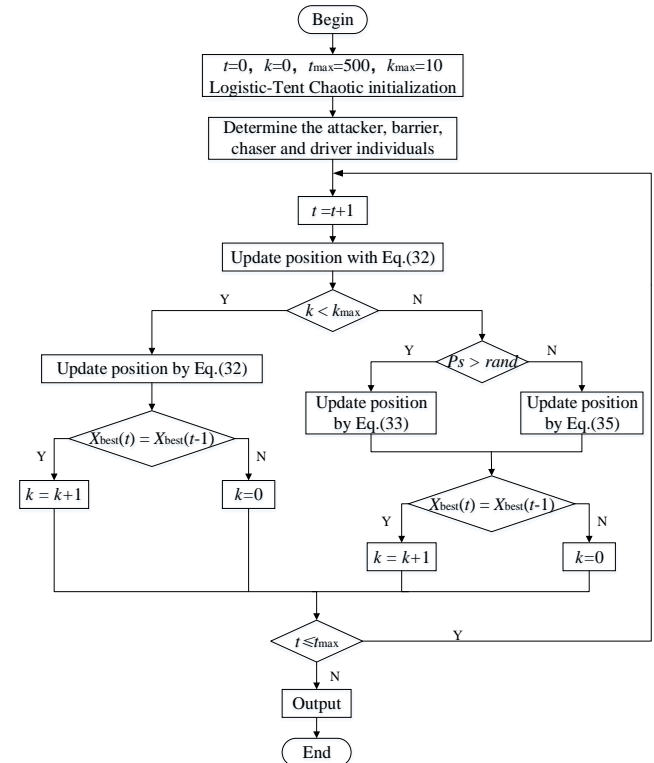


Fig. 1. The flow chart of IChOA

C. Test for IChOA

In this paper, 13 benchmark test functions with different characteristics in TABLE I are selected for simulation experiment analysis to verify the effectiveness and robustness of the proposed algorithm. TABLE I presents the basic information of the 13 benchmark test functions in detail, including mathematical expressions, definition domains and optimal values, among which F1-F7 are continuous unimodal functions to test the convergence

accuracy of the algorithm, and F8-F13 are continuous multimodal functions with multiple local extremes to test the global search capability of the algorithm.

In order to test the optimization performance of IChOA objectively and fairly, the basic parameters of the algorithm are set the same: population size $N=50$, number of iterations $K_{\max}=500$, and spatial dimension $D=30$. On the other hand, each group of simulations are operated 50 times independently so as to eliminate the influence of fortuitous element on experimental results. And the experimental data obtained are arranged in TABEL I.

TABEL I
THE BENCHMARK FUNCTIONS

| Name | Function | Dim | Domain | f_{\min} |
|------|--|-----|--------------|---------------|
| F1 | $f_1 = \sum_{i=1}^N x_i^2$ | 30 | [-100,100] | 0 |
| F2 | $f_2 = \sum_{i=1}^N x_i + \prod_{i=1}^N x_i $ | 30 | [-10,10] | 0 |
| F3 | $f_3 = \sum_{i=1}^N (\sum_{j=1}^i x_j)^2$ | 30 | [-100,100] | 0 |
| F4 | $f_4 = \max_i \{ x_i , 1 \leq i \leq N\}$ | 30 | [-100,100] | 0 |
| F5 | $f_5 = \sum_{i=1}^{N-1} [100(x_{i+1} - x_i^2)^2 + (x_i - 1)^2]$ | 30 | [-30,30] | 0 |
| F6 | $f_6 = \sum_{i=1}^N (x_i + 0.5)^2$ | 30 | [-100,100] | 0 |
| F7 | $f_7 = \sum_{i=1}^N ix_i^4 + \text{random}[0,1)$ | 30 | [-1.28,1.28] | 0 |
| F8 | $f_8 = \sum_{i=1}^N -x_i \sin(\sqrt{ x_i })$ | 30 | [-500,500] | -418.9829×Dim |
| F9 | $f_9 = \sum_{i=1}^N [x_i^2 - 10 \cos(2\pi x_i) + 10]$ | 30 | [-5.12,5.12] | 0 |
| F10 | $f_{10} = -20 \exp(-0.2 \sqrt{\frac{1}{N} \sum_{i=1}^N x_i^2}) - \exp(\frac{1}{N} \sum_{i=1}^N \cos(2\pi x_i)) + 20 + e$ | 30 | [-32,32] | 0 |
| F11 | $f_{11} = \frac{1}{4000} \sum_{i=1}^N x_i^2 - \prod_{i=1}^N \cos(\frac{x_i}{\sqrt{i}}) + 1$ | 30 | [-600,600] | 0 |
| F12 | $f_{12} = \frac{\pi}{N} \{10 \sin(\pi y_i) + \sum_{i=1}^{N-1} (y_i - 1)^2 [1 + 10 \sin^2(\pi y_{i+1})] + (y_N - 1)^2\} + \sum_{i=1}^N u(x_i, 10, 100, 4)$ $y_i = 1 + \frac{x_i + 1}{4}$ $u(x_i, a, k, m) = \begin{cases} k(x_i - a)^m & x_i > a \\ 0 & -a < x_i < a \\ k(-x_i - a)^m & x_i < -a \end{cases}$ | 30 | [-50,50] | 0 |
| F13 | $f_{13} = 0.1 \{ \sin^2(3\pi x_1) + \sum_{i=1}^N (x_i - 1)^2 [1 + \sin^2(3\pi x_i + 1)] + (x_N - 1)^2 [1 + \sin^2(2\pi x_N)] \} + \sum_{i=1}^N u(x_i, 5, 100, 4)$ | 30 | [-50,50] | 0 |

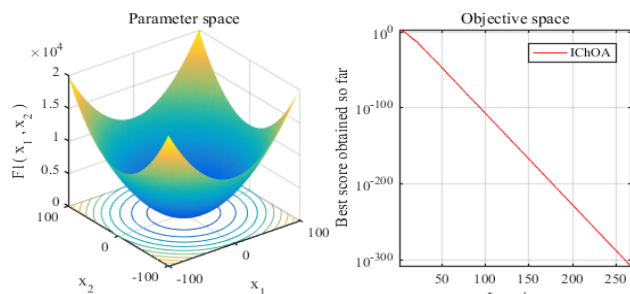


Fig. 2.The 2-D view and convergence curve of F1

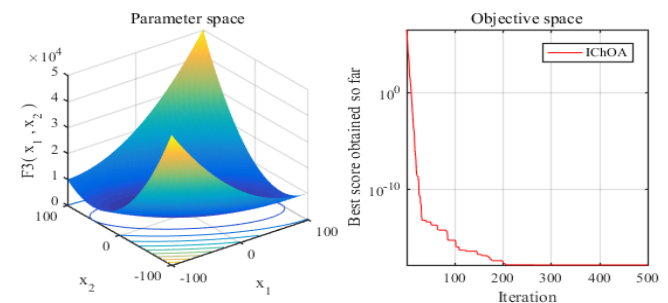


Fig. 4.The 2-D view and convergence curve of F3

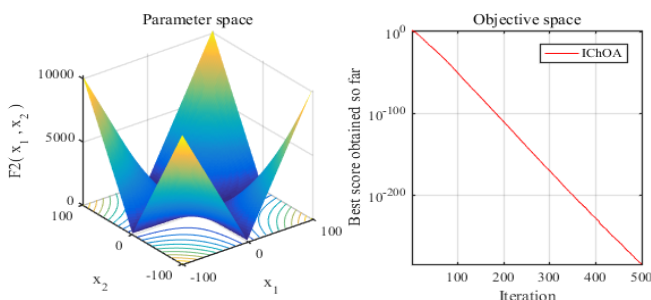


Fig. 3.The 2-D view and convergence curve of F2

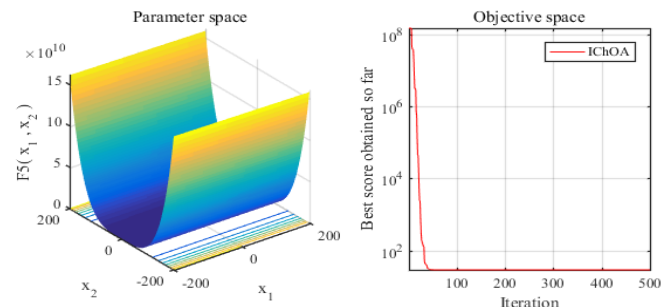


Fig. 5.The 2-D view and convergence curve of F5

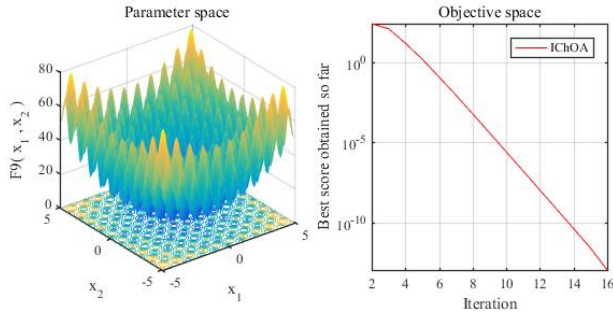


Fig. 6. The 2-D view and convergence curve of F9

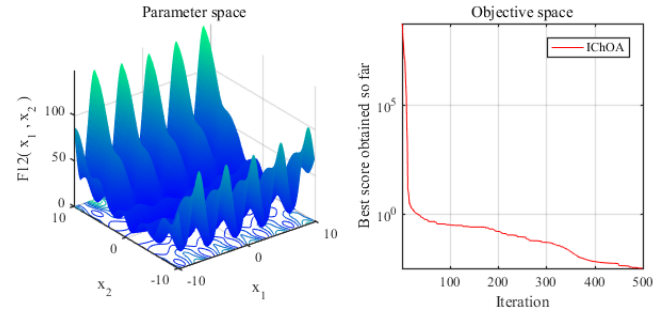


Fig. 8. The 2-D view and convergence curve of F12

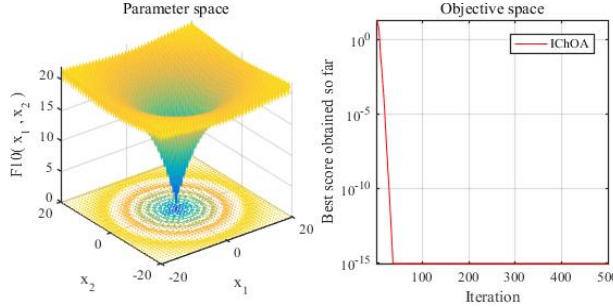


Fig. 7. The 2-D view and convergence curve of F10

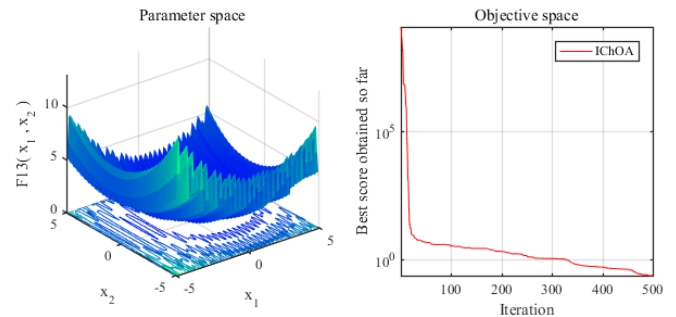


Fig. 9. The 2-D view and convergence curve of F13

 TABLE II
THE RESULTS OF 13 BENCHMARK FUNCTIONS

| Function | IChOA | | | | ChOA | | | |
|----------|-----------|-----------|-----------|----------|-----------|-----------|-----------|----------|
| | Min. | Max. | Avg. | Std. | Min. | Max. | Avg. | Std. |
| F1 | 0.00E+00 | 5.71E-57 | 1.67E-58 | 8.47E-58 | 4.71E-26 | 8.28E-21 | 4.54E-22 | 1.46E-21 |
| F2 | 7.62E-302 | 2.47E-30 | 1.94E-31 | 5.23E-31 | 7.65E-18 | 3.98E-15 | 5.46E-16 | 8.33E-16 |
| F3 | 7.42E-69 | 1.39E-17 | 4.99E-19 | 2.46E-18 | 1.29E-07 | 4.00E-01 | 1.11E-02 | 5.63E-02 |
| F4 | 9.01E-34 | 6.51E-10 | 2.49E-11 | 9.97E-11 | 9.64E-08 | 8.08E-05 | 8.60E-06 | 1.62E-05 |
| F5 | 2.55E+01 | 2.83E+01 | 2.69E+01 | 7.06E-01 | 2.58E+01 | 2.88E+01 | 2.78E+01 | 7.76E-01 |
| F6 | 2.68E+01 | 1.22E-01 | 7.82E-01 | 3.14E-01 | 2.93E-01 | 1.26E+00 | 8.97E-01 | 3.56E-01 |
| F7 | 3.34E-05 | 9.60E-04 | 5.07E-04 | 2.21E-04 | 5.49E-05 | 2.17E-03 | 5.94E-04 | 4.63E-04 |
| F8 | -6.94E+03 | -5.65E+03 | -6.13E+03 | 3.11E+02 | -6.89E+03 | -4.82E+03 | -5.71E+03 | 3.22E+02 |
| F9 | 0.00E+00 | 0.00E+00 | 0.00E+00 | 0.00E+00 | 0.00E+00 | 4.43E-11 | 1.39E-12 | 6.65E-12 |
| F10 | 8.88E-16 | 4.44E-15 | 2.52E-15 | 1.77E-15 | 4.35E-14 | 6.18E-10 | 2.68E-11 | 9.75E-11 |
| F11 | 0.00E+00 | 0.00E+00 | 0.00E+00 | 0.00E+00 | 0.00E+00 | 0.00E+00 | 0.00E+00 | 0.00E+00 |
| F12 | 3.04E-05 | 8.91E-03 | 2.17E-03 | 2.07E-03 | 3.11E-02 | 8.38E-02 | 4.46E-02 | 1.26E-02 |
| F13 | 1.49E-01 | 9.71E-01 | 3.19E-01 | 1.54E-01 | 7.79E-01 | 1.37E+00 | 1.07E+00 | 1.70E-01 |

IV. THE APPLICATION OF IChOA FOR STHS PROBLEM

A. Structure of initialization

The initialization population of the STHS problem corresponds to the chimp individuals of IChOA, each of which contains information on several variables. The structure of the initial population consists of the discharge of each hydropower plant and the output power of each thermal plant at each time period. A single chimp individual X_d ($d=1, 2, \dots, NP$) is initialized in the following form.

$$X_d = \begin{bmatrix} Q_{11}^{hp} & Q_{21}^{hp} & \dots & Q_{N_h 1}^{hp} & P_{11}^{tp} & P_{21}^{tp} & \dots & P_{N_s 1}^{tp} \\ Q_{12}^{hp} & Q_{22}^{hp} & \dots & Q_{N_h 2}^{hp} & P_{12}^{tp} & P_{22}^{tp} & \dots & P_{N_s 2}^{tp} \\ \vdots & \vdots & \dots & \vdots & \vdots & \vdots & \dots & \vdots \\ Q_{1T}^{hp} & Q_{2T}^{hp} & \dots & Q_{N_h T}^{hp} & P_{1T}^{tp} & P_{2T}^{tp} & \dots & P_{N_s T}^{tp} \end{bmatrix} \quad (38)$$

The generation of the initial population is strictly limited to the feasible region, thus avoiding emergence of default solutions.

$$\begin{cases} Q_{jt}^{hp} = Q_{j,\min}^{hp} + m_m (Q_{j,\max}^{hp} - Q_{j,\min}^{hp}) \\ P_{it}^{tp} = P_{i,\min}^{tp} + m_n (P_{i,\max}^{tp} - P_{i,\min}^{tp}) \end{cases} \quad (39)$$

where m_m and m_n are the two of the chaotic sequence generated by Logistic-Tent chaos.

B. Constraints handing

When IChOA is applied to solve the STHS problem, it is extremely easy to violate the constraints due to the complexity of the STHS structure. The occurrence of such a phenomenon will lead to an incalculable disaster, so constraint handing is required to make it strictly satisfy the constraints and ensure the feasibility of the scheduling scheme.

1) Discharge volume limitation

$$Q_{jt}^{hp} = \begin{cases} Q_{j,\min}^{hp} & (Q_{jt}^{hp} < Q_{j,\min}^{hp}) \\ Q_{jt}^{hp} & (Q_{j,\min}^{hp} \leq Q_{jt}^{hp} \leq Q_{j,\max}^{hp}) \\ Q_{j,\max}^{hp} & (Q_{jt}^{hp} > Q_{j,\max}^{hp}) \end{cases} \quad (40)$$

2) Reservoir volume limitation

$$V_{jt}^{hp} = \begin{cases} V_{j,\min}^{hp} & (V_{jt}^{hp} < V_{j,\min}^{hp}) \\ V_{jt}^{hp} & (V_{j,\min}^{hp} \leq V_{jt}^{hp} \leq V_{j,\max}^{hp}) \\ V_{j,\max}^{hp} & (V_{jt}^{hp} > V_{j,\max}^{hp}) \end{cases} \quad (41)$$

3) Output power limitation

$$P_{it}^{lp} = \begin{cases} P_{i,\min}^{lp} & (P_{it}^{lp} < P_{i,\min}^{lp}) \\ P_{it}^{lp} & (P_{i,\min}^{lp} \leq P_{it}^{lp} \leq P_{i,\max}^{lp}) \\ P_{i,\max}^{lp} & (P_{it}^{lp} > P_{i,\max}^{lp}) \end{cases} \quad (42)$$

The output power constraint treatment strategy for hydropower plants also emulates Eq.(42).

4) Dynamic reservoir balance

In the scheduling optimization process, the initial and final values of the reservoir volume capacity must meet the conditions given by the system while maintaining water dynamic balance, which will be a complex process to handle. Therefore, a graded optimization strategy is employed to deal with dynamic reservoir balance, and the pseudo code is shown in Fig. 10. The process is divided into two phases: firstly, when the violation of the reservoir volume is less than the defined parameter value, named $\varepsilon_{\text{error}}$, the period with the largest margin value undertakes the violation; secondly, if the violation of the reservoir volume is greater than the set parameter value, the average method is used to divide the violation volume into each interval equally.

5) Dynamic power balance

The constraint processing on the power balance of the power system is handled after the above adjustment, which will not affect previous operation. The processing method of power balance still adopts the graded optimization strategy based on economy, which is divided into two steps: firstly, when the violation of the power balance is less than the defined parameter value, named $\varepsilon_{\text{error}}$, the thermal plant with the smallest economic index undertakes the violation; secondly, if the violation of the power balance is greater than the set parameter value, the average method is used to divide the violation volume into each thermal plant equally. In addition, the pseudo code of constraints handling for thermal power balance is presented in Fig. 11.

```

Begin
For  $j = 1 : N_h$ 
     $Iter = 0$ 

     $Q_{jb}^{hp} = V_{j,\text{initial}}^{hp} - V_{j,\text{final}}^{hp} + \sum_{t=1}^T I_{jt}^{hp} + \sum_{t=1}^T \sum_{m=1}^{R_j} (Q_{m(t-\tau_m)}^{hp}) - \sum_{t=1, t \neq b}^T Q_{jt}^{hp}$ 

    Check  $Q_{jb}^{hp}$ 

     $\Delta V_{\text{error}} = V_{j,\text{initial}}^{hp} - V_{j,\text{final}}^{hp} + \sum_{t=1}^T I_{jt}^{hp} + \sum_{t=1}^T \sum_{m=1}^{R_j} (Q_{m(t-\tau_m)}^{hp}) - \sum_{t=1}^T Q_{jt}^{hp}$ 

    While  $|\Delta V_{\text{error}}| < \varepsilon_{\text{error}}$  and  $Iter < Iter_{\text{max}}$ 
        Calculate  $\Delta Q_{jt}^{hp}$  from  $t = 1 : T$ 
        Choose  $l$  with the largest adjustable margin
         $Q_{jl}^{hp} = Q_{jl}^{hp} + \Delta V_{\text{error}}$ ; Check  $Q_{jl}^{hp}$ ;
         $Iter = Iter + 1$ 
    End while
    While  $|\Delta V_{\text{error}}| \geq \varepsilon_{\text{error}}$  and  $Iter < Iter_{\text{max}}$ 
         $avg \Delta V_{\text{error}} = \Delta V_{\text{error}} / T$ 
        For  $t = 1 : T$ 
             $Q_{jt}^{hp} = Q_{jt}^{hp} + avg \Delta Q_{\text{error}}$ ; Check  $Q_{jt}^{hp}$ ;
        End for
         $Iter = Iter + 1$ 
    End while
End for
End
    
```

Fig. 10.Pseudo code of constraints handling for reservoir capacity

```

Begin
For  $t = 1 : T$ 
     $Iter = 0$ 

     $\Delta P_t = P_{Dt} + P_{Lt} - \sum_{i=1}^{N_s} P_{it}^{lp} - \sum_{j=1}^{N_h} P_{jt}^{hp}$ 

    While  $|\Delta P_t| < \varepsilon_{\text{error}}$  and  $Iter < Iter_{\text{max}}$ 
        Calculate  $\alpha_{it} = \frac{F_c(P_{it}^{k+1}) - F_c(P_{it}^k)}{P_{it}^{k+1} - P_{it}^k}$  from  $i = 1 : N_s$ 
        List  $\alpha_{it}$  in ascending order and choose  $z$  with the smallest index
         $P_{zt}^{lp} = P_{zt}^{lp} + \Delta P_t$ ; Check  $P_{zt}^{lp}$ 
         $Iter = Iter + 1$ 
    End while
    While  $|\Delta P_t| \geq \varepsilon_{\text{error}}$  and  $Iter < Iter_{\text{max}}$ 
         $avg \Delta P_t = \Delta P_t / N_s$ 
        For  $i = 1 : N_s$ 
             $P_{it}^{lp} = P_{it}^{lp} + avg \Delta P_t$ ; Check  $P_{it}^{lp}$ ;
        End for
         $Iter = Iter + 1$ 
    End while
End for
End
    
```

Fig. 11.Pseudo code of constraints handling for thermal power balance

V. SIMULATION RESULTS AND DISCUSSION

Three standard test systems including four cases have been selected for simulation experiments to validate the effectiveness of the proposed IChOA for addressing the STHS problem. The entire scheduling period is one day with one-hour interval. All simulation experiments are implemented on a PC (3GHz and 16GB) with MATLAB-2016a installed.

A. Test system I

The test system I comprises of four hydropower plants and one thermal plant, with no consideration of the valve point effect and the transmission loss. The system data of this test refers to [34]. In this case, the results of the experiments conducted 50 times have been summarized as follows. The convergence curve is shown in Fig. 12, the result obtained by IChOA algorithm is superior to the original ChOA and PSO. Moreover, the reservoir capacity volume is denoted in Fig. 13, we can see clearly that all hydropower plants satisfy the given constraints. The optimal output scheme obtained in system I is shown in TABEL VII and drawn in Fig. 14, which precisely shows the power output of each plant. Fig. 15 clearly reflects the relationship between output power and load demand, satisfying load balance constraints.

In the meanwhile, TABEL III and Fig. 16 illustrate the fuel costs comparison between IChOA and other literature algorithms, including ChOA, NLP [5], DE [12], LWPSO [13], RCGA [22], RQEA [35], QEA [35] and RE-GA [36]. It can be seen obviously from TABEL III that the minimum, maximum and average fuel costs obtained by the proposed IChOA are 922916.97(\$), 923786.08(\$), and 923413.20(\$), respectively, and all are lower than the costs obtained by other methods. For instance, compared to RQEA, IChOA reduces by 718.53(\$), 3171.31(\$), and 1579.26(\$), in terms of the minimum, maximum and average fuel costs respectively, saving the cost of power generation. Hence, it is demonstrated that the proposed IChOA has a

significant advantage over other methods in solving the STHS problem.

TABEL III
THE COST COMPARISON WITH OTHER METHODS

| Method | Fuel cost (\$) | | |
|--------|------------------|-----------|-----------|
| | Min. | Max. | Avg. |
| ICHOA | 922916.97 | 923786.08 | 923413.20 |
| RQEA | 923634.53 | 926957.39 | 924992.46 |
| RCGA | 923966.29 | 924232.07 | 924108.73 |
| DE | 923991.08 | 928395.84 | 925157.28 |
| RE-GA | 924159.60 | 925613.60 | 924880.40 |
| NLP | 924249.48 | NA | NA |
| ChOA | 924456.17 | 926575.68 | 924987.13 |
| LWPSO | 925383.80 | 927240.10 | 926352.80 |
| QEA | 926538.29 | 930484.13 | 928426.95 |

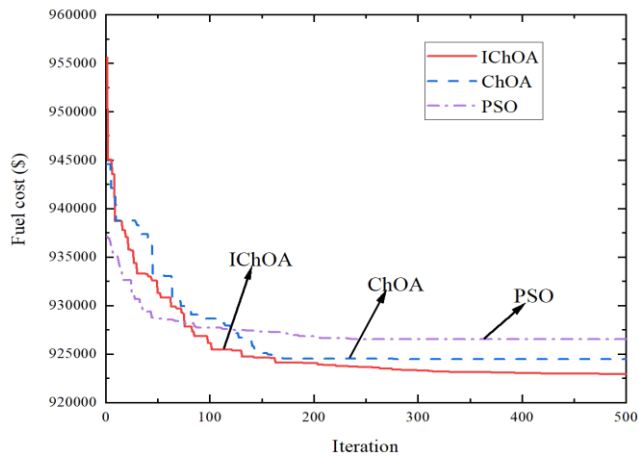


Fig. 12. The convergence curve of system I

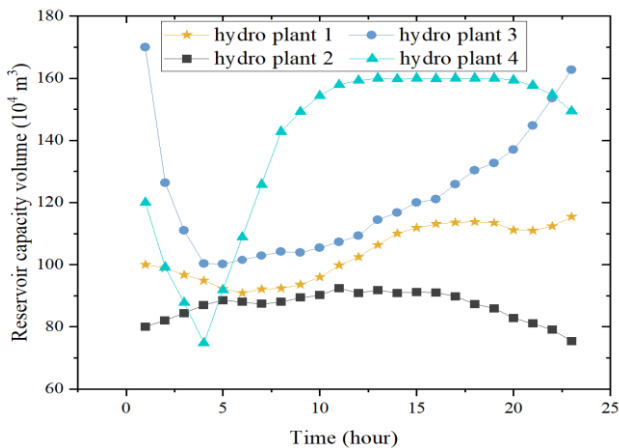


Fig. 13. The reservoir capacity volume of system I

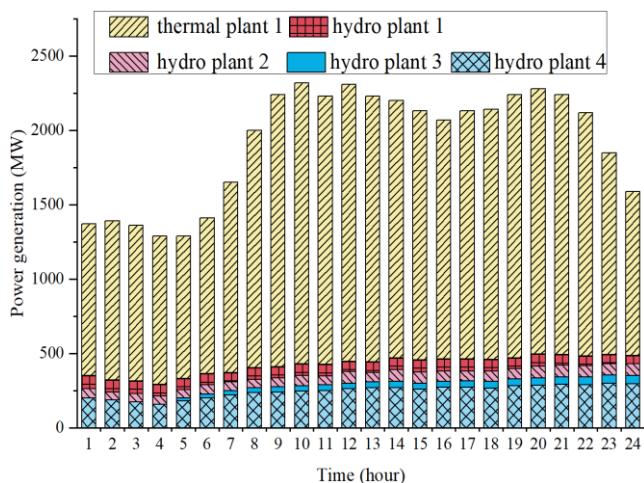


Fig. 14. The power generation of each plant of system I

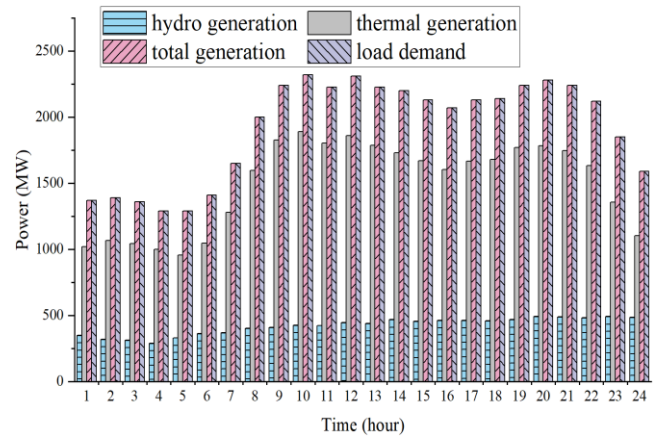


Fig. 15. The power generation and load demand of system I

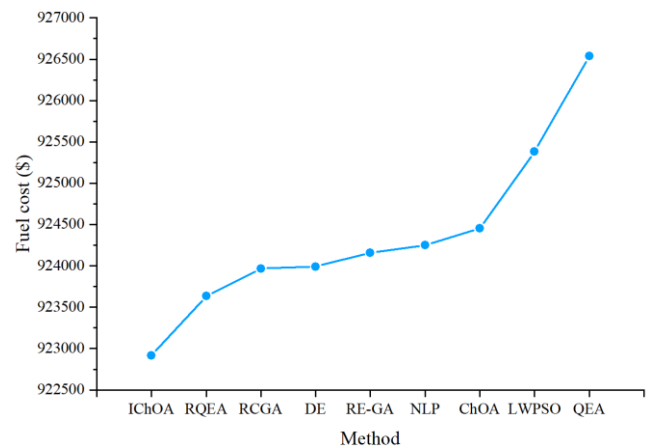


Fig. 16. The cost comparison with other methods

B. Test system II

The test system II is composed of four hydropower plants and three thermal power plants, which is subdivided into two cases according to whether transmission loss is considered or not. The detailed data of test system II is retrieved from the reference [37].

1) Case 1 of system II

Only the valve point effect of the power system is considered in case 1, and the experiments have been repeated 50 times. As shown clearly in Fig. 17, IChOA has the best convergence characteristic and the lowest fuel cost, and all satisfy the reservoir constraints during the scheduling period according to Fig. 18. In addition, the specific output power of each power plant is displayed clearly in Fig. 19, and the power constraint is strictly satisfied during the optimization search. TABEL VIII shows the optimal scheduling scheme of hydropower plants and thermal plants with the best convergence result after 50 repeated experiments. It can be seen intuitively from Fig. 20 that the total output power corresponding to each time period is equal to the load demand, indicating that the two are always in a state of dynamic balance.

Furthermore, TABEL IV and Fig. 21 present the fuel costs comparison between IChOA and other algorithms, including ChOA, MCDE [17], RCGA-AFSA [22], ALO [38], DNLP [39], RCCRO [40], DGSA [41] and QTLBO [42]. It can be seen intuitively from TABEL IV that the minimum, maximum and average fuel costs obtained by the proposed IChOA are 40389.01(\$), 40803.91(\$), and 40567.60(\$), and they are all lower than the

costs obtained by other methods in varying degrees, which indicates that the proposed IChOA is more competitive in dealing with the STHS problem and can achieve higher economic benefits.

TABEL IV
THE COST COMPARISON WITH OTHER METHODS

| Method | Fuel cost (\$) | | |
|-----------|-----------------|----------|----------|
| | Min. | Max. | Avg. |
| IChOA | 40389.01 | 40803.91 | 40567.60 |
| ChOA | 40641.29 | 41211.72 | 40805.52 |
| ALO | 40780.05 | 41094.34 | 40905.83 |
| RCGA-AFSA | 40913.83 | 41235.73 | 41362.58 |
| MCDE | 40945.75 | 41977.04 | 41380.54 |
| DNLP | 41101.74 | NA | NA |
| RCCRO | 41497.85 | 41498.21 | 41502.37 |
| DGSA | 41751.15 | 41989.02 | 41821.49 |
| QTLBO | 42187.49 | 42202.75 | 42193.46 |

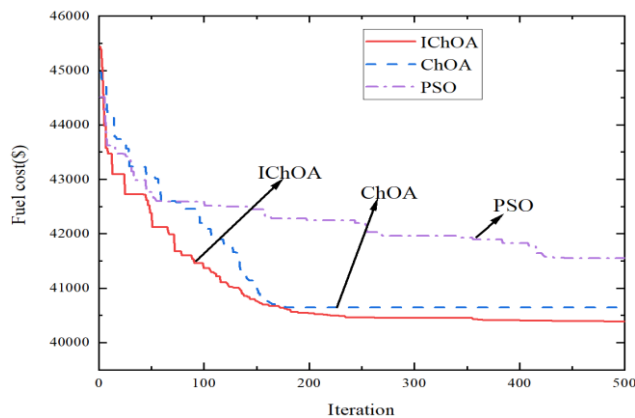


Fig. 17. The convergence curve of case 1 in system II

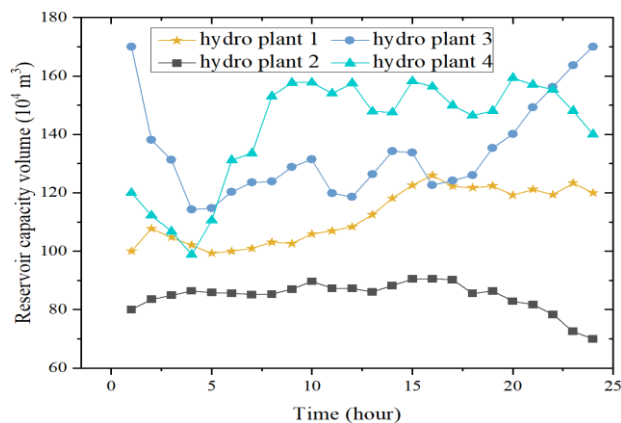


Fig. 18. The reservoir capacity volume of case 1 in system II

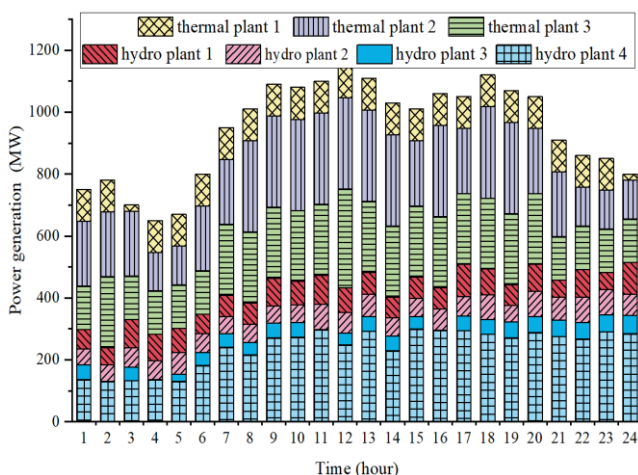


Fig. 19. The power generation of each plant of case 1 in system II

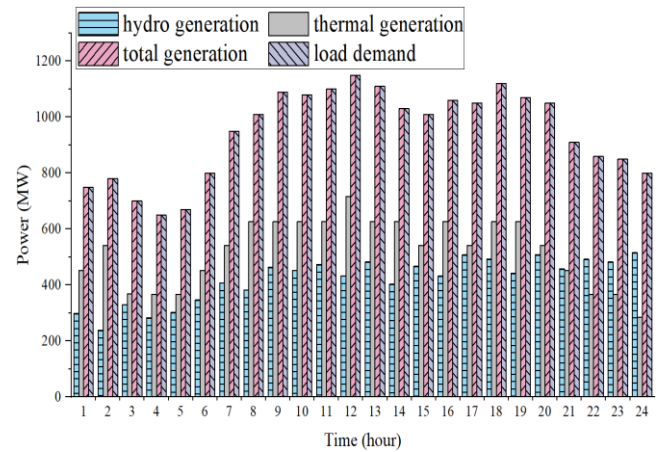


Fig. 20. The power generation and load demand of case 1 in system II

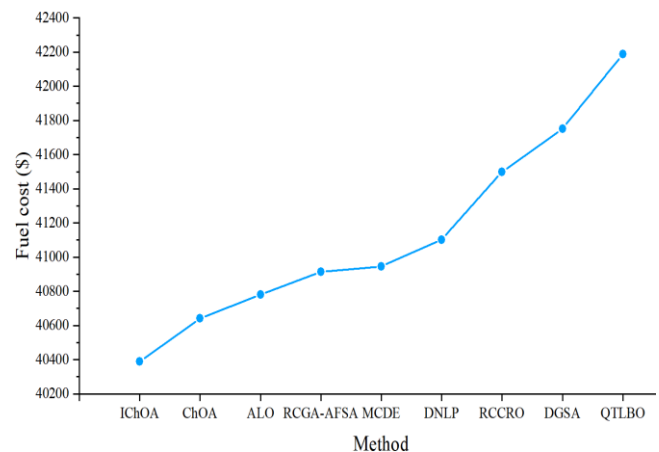


Fig. 21. The cost comparison with other methods

2) Case 2 of system II

The case 2 of system II takes both valve point effect and transmission loss into account, which makes the nonlinearity of the STHS problem more prominent and difficult to solve. Fig. 22 presents the convergence property curves of the optimal results obtained by IChOA, ChOA, and PSO by conducting 50 repetitions of experiments. It can be seen that IChOA has better accuracy of global optimization search holistically. The reservoir volume distribution of the hydropower plants during the whole dispatch period is plotted in Fig. 23, and no constraint violation occurs in each reservoir during this process. In addition, Fig. 24 and TABEL IX illustrate the output power distribution of each power plant in detail. It can be seen from Fig. 25 that the total output power of the power system is greater than the load demand, and the extra output power makes up for the transmission loss, which is a normal and reasonable phenomenon.

What's more, the optimal fuel cost calculated by IChOA has been compared with the results of ChOA, MCDE [17], RCGA-AFSA [22], ALO [38], DNLP [39], GSA [41], MDNLP [43], QOGSO [44] and GSO [44], including the minimum, maximum and average fuel cost, which as shown in TABEL V and Fig. 26. The minimum, maximum and average fuel costs obtained by the proposed method are 41094.39(\$), 41936.36(\$), and 41560.20(\$), respectively. The above results demonstrate that the complexity of the system increases when loss is considered, but the proposed IChOA is still significant for the optimization of the STHS problem.

TABEL V
THE COST COMPARISON WITH OTHER METHODS

| Method | Fuel cost (\$) | | |
|-----------|-----------------|----------|----------|
| | Min. | Max. | Avg. |
| IchOA | 41094.39 | 41936.36 | 41560.20 |
| MDNLP | 41183.00 | 41994.00 | 41595.00 |
| DNLP | 41350.56 | NA | NA |
| ChOA | 41448.04 | 42440.49 | 41702.02 |
| MCDE | 41586.18 | 42365.84 | 42022.67 |
| RCGA-AFSA | 41707.96 | 41894.63 | 41894.63 |
| GSA | 42032.35 | 42561.53 | 42292.12 |
| QOGSO | 42120.02 | 42145.37 | 42130.15 |
| GSO | 42316.39 | 42379.18 | 42339.35 |
| ALO | 42833.91 | 42900.19 | 42867.31 |

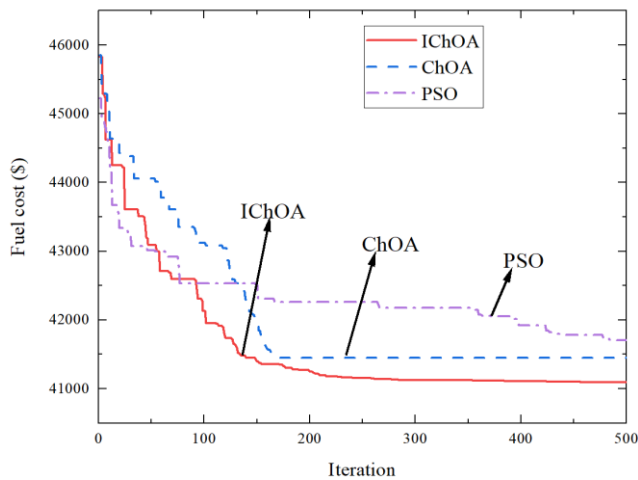


Fig. 22.The convergence curve of case 2 in system II

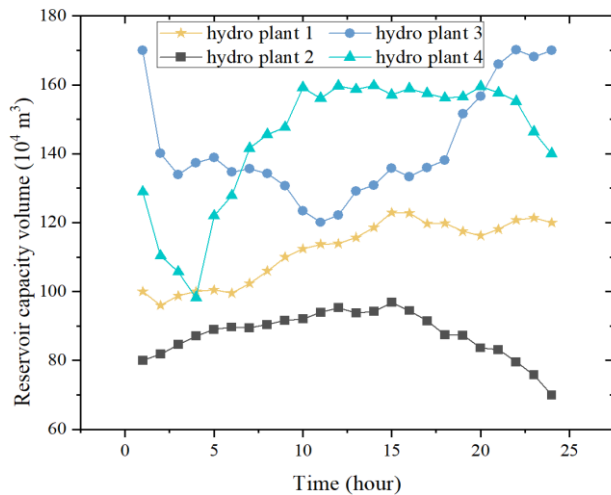


Fig. 23.The reservoir capacity volume of case 2 in system II

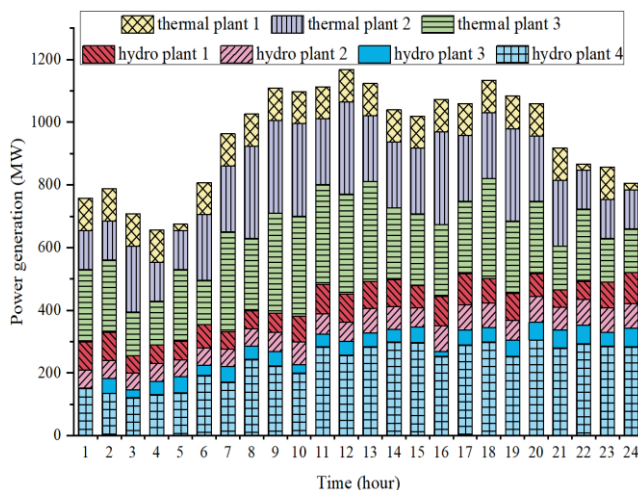


Fig. 24.The power generation of each plant of case 2 in system II

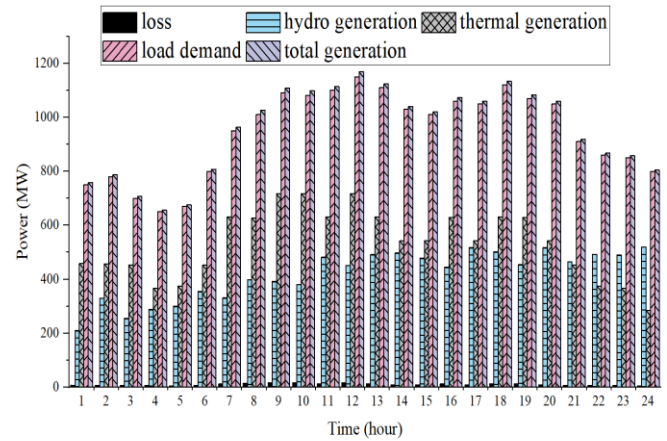


Fig. 25.The power generation and load demand of case 2 in system II

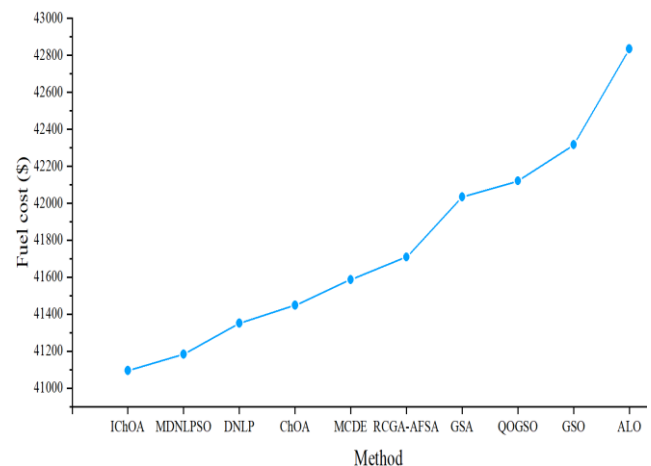


Fig. 26.The cost comparison with other methods

C. Test system III

The test system III consists of four hydropower plants and ten thermal power plants without considering the system transmission loss, whose scale is larger and more sophisticated than the previous test systems. The higher dimensional test system makes the STHS problem more intractable. The detailed data of test system III is retrieved from the reference [2].

Likewise, the experiment has also been performed 50 times. As shown clearly in Fig. 27, the convergence speed of IchOA is faster, converging when the number of iteration is close to 150, and the quality of the global optimal solution obtained is much higher compared with ChOA and PSO. Fig. 28 reflects the real-time changing trend of storage capacity of various reservoirs within 24 hours without any default. The power generation of each plant is revealed clearly in Fig. 29. Besides, the optimal scheduling scheme of hydropower plants and thermal plants are represented in TABEL X and TABEL XI respectively. Likewise, the output power and load demand at each time period shown in Fig. 30 satisfy the equality relationship within the scheduling period, indicating that no power constraint violation occurs and IchOA can effectively solve the STHS problem.

Additionally, the optimal fuel cost calculated by IchOA has been compared with the results of ChOA, MCDE [17], ALO [38], ORCCRO [40], QOGSO [44] and GSO [44], IPCSO [2], SOS [45] and SPPSO [46], including the minimum, maximum and average fuel cost, which as shown

in TABEL VI and Fig. 31. The minimum, maximum and average fuel costs obtained by the proposed method are 161409.60(\$), 163630.23(\$), and 162141.40(\$), respectively. Experiments have shown that the fuel cost obtained by ICHOA is lower than that of most methods, with higher economy and stronger search capability. It robustly proves that the proposed ICHOA has a great competitiveness and provides a new solution idea for solving the STHS problem.

TABEL VI
THE COST COMPARISON WITH OTHER METHODS

| Method | Fuel cost (\$) | | |
|--------|------------------|-----------|-----------|
| | Min. | Max. | Avg. |
| ICHOA | 161409.60 | 162630.23 | 162141.40 |
| ALO | 161353.97 | 161363.06 | 161356.17 |
| ChOA | 162658.00 | 163264.47 | 163024.70 |
| IPCSO | 162714.00 | 162953.00 | 162813.00 |
| SOS | 162834.38 | 163147.87 | 162846.92 |
| ORCCRO | 163066.03 | 163134.54 | 163068.77 |
| MCDE | 165330.70 | 167060.60 | 166116.40 |
| SPPSO | 167710.56 | 170879.30 | 168688.92 |
| QOGSO | 170293.21 | 170349.34 | 170321.57 |
| GSO | 170511.26 | 170586.91 | 170547.56 |

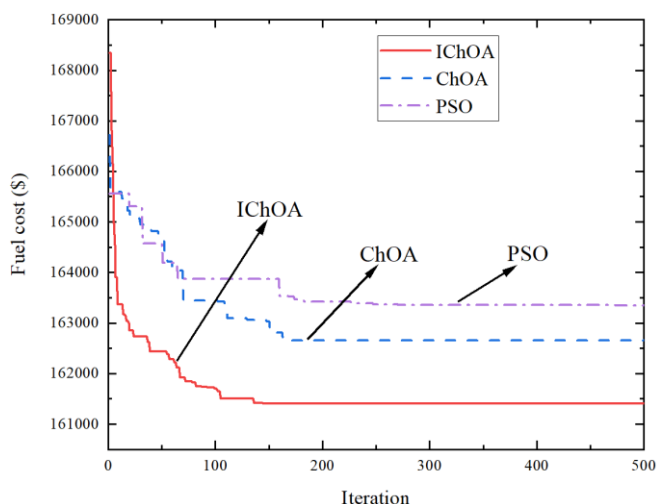


Fig. 27. The convergence curve of system III

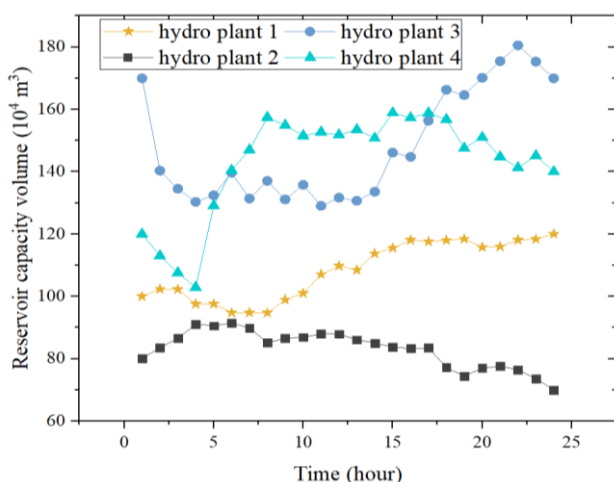


Fig. 28. The reservoir capacity volume of system III

Abbreviations Comment

| | |
|-------|---------------------------------------|
| STHS | short-term hydrothermal scheduling |
| ChOA | chimp optimization algorithm |
| ICHOA | improved chimp optimization algorithm |
| PSO | particle swarm algorithm |
| GSA | gravitational search algorithm |
| LP | linear programming |

| | |
|-----------|---|
| NLP | nonlinear programming |
| DP | dynamic programming |
| MIP | mixed integer programming |
| LR | Lagrange relaxation |
| GS | gradient search techniques |
| GA | genetic algorithm |
| DE | differential evolution |
| HNN | Hopfield neural network |
| ABC | artificial bee colony algorithm |
| GOA | grasshopper optimization algorithm |
| MCDE | modified chaotic differential evolution |
| OGB-GA | optimal gamma based genetic algorithm |
| MCSA | modified cuckoo search algorithm |
| MSGO | modified social group optimization |
| APSO | accelerated particle swarm optimization |
| RCGA-AFSA | hybrid of real coded genetic algorithm and artificial fish swarm algorithm |
| WOA | whale optimization algorithm |
| GWO | gray wolf optimizer |
| NGS-WOA | improved whale optimization algorithm based on nonlinear adaptive weight and golden sine operator |
| TGWO | improved grey wolf optimizer based on tracking mode |
| SGWO | improved grey wolf optimizer based on seeking mode |
| LWPSO | local vision of PSO with inertia weight |
| RCGA | real coded genetic algorithm |
| RQEA | real-coded quantum-inspired evolutionary algorithm |
| QEA | quantum-inspired evolutionary algorithm |
| ALO | ant lion optimization |
| DNLP | dynamic non-linear programming |
| RCCRO | real coded chemical reaction based optimization |
| DGSA | disruption based gravitational search algorithm |
| QTLBO | quasi-oppositional teaching learning based optimization |
| MDNLPSO | modified dynamic neighborhood learning based particle swarm optimization |
| QOGSO | quasi-oppositional group search optimization |
| GSO | Quasi-oppositional group search optimization |
| ORCCRO | oppositional real coded chemical reaction based optimization |
| IPCSO | novel two-swarm based PSO search strategy |
| SOS | symbiotic organisms search algorithm |
| SPPSO | small population-based particle swarm optimization |

VI. CONCLUSION

In this paper, an improved chimp optimization algorithm (ICHOA) incorporating various improvements is proposed and successfully applied to the non-linear, non-convex and high-dimensional STHS problem. The effectiveness of the improved method is verified by three standard complex systems including four test cases. Additionally, the minimum, maximum and average fuel costs obtained by the proposed ICHOA have noticeable advantages compared with a great number of methods from other literature. For instance, in case 2 of system II, the minimum, maximum

and average fuel costs obtained by IChOA are 41094.39(\$), 41936.36(\$), 41560.20(\$), respectively, and they save 491.79(\$), 429.48(\$), 462.47(\$), respectively compared with the ones of MCDE. Meanwhile, the convergence result of IChOA has the advantages of superior performance, high precision and high robustness. Furthermore, numerous charts illustrate that the whole process does not violate the constraints, thereby certifying the effectiveness of the constraint handling strategy. In a nutshell, it is evident that the proposed IChOA is reasonable and effective, which provides a new idea for the solution of the increasingly challenging STHS problem and the large-scale constrained optimization problem.

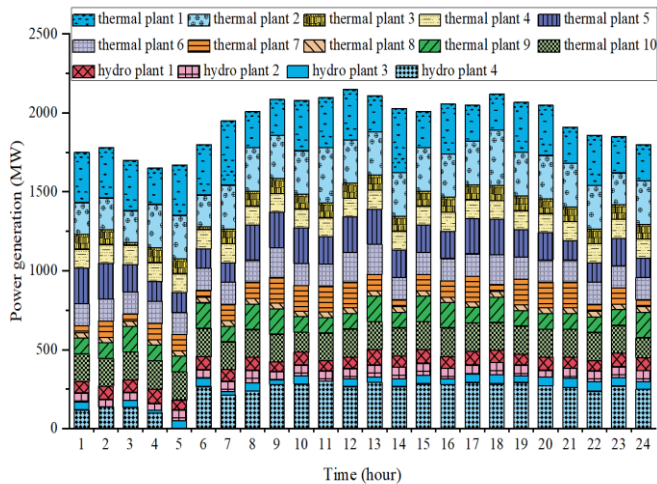


Fig. 29. The power generation of each plant of system III

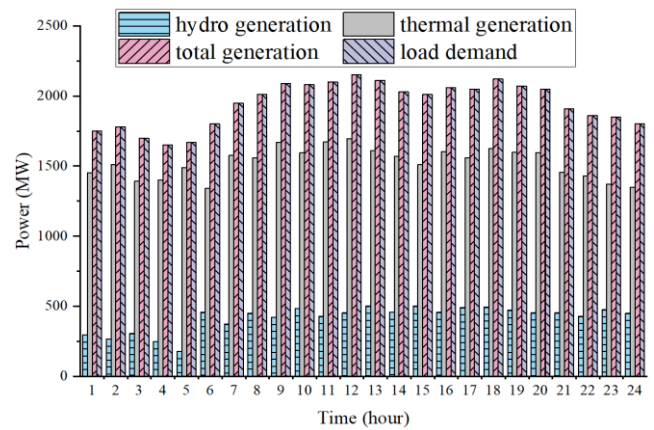


Fig. 30. The power generation and load demand of system III

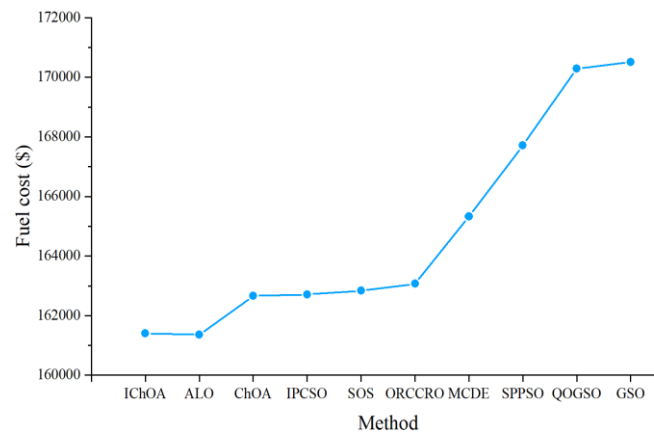


Fig. 31. The cost comparison with other methods

TABEL VII
THE OPTIMAL SCHEDULING SOLUTION OF SYSTEM I

| Time (hour) | Hydro discharge (10^4 m^3) | | | | Hydro generation (MW) | | | | Thermal generation (MW) | P_{total} (MW) | P_{load} (MW) |
|----------------|--|----------|----------|----------|-----------------------|----------|----------|----------|----------------------------|----------------------------|---------------------------|
| | Q_{h1} | Q_{h2} | Q_{h3} | Q_{h4} | P_{h1} | P_{h2} | P_{h3} | P_{h4} | | | |
| 1 | 10.66 | 7.87 | 30.00 | 13.00 | 88.59 | 61.31 | 0.00 | 200.09 | 1020.01 | 1370.00 | 1370.00 |
| 2 | 9.45 | 6.09 | 30.00 | 13.00 | 82.96 | 50.84 | 0.00 | 187.76 | 1068.44 | 1390.00 | 1390.00 |
| 3 | 10.16 | 6.64 | 30.00 | 13.00 | 85.50 | 55.99 | 0.00 | 173.74 | 1044.77 | 1360.00 | 1360.00 |
| 4 | 8.85 | 6.37 | 30.00 | 13.00 | 78.40 | 55.60 | 0.00 | 156.79 | 999.21 | 1290.00 | 1290.00 |
| 5 | 8.58 | 6.47 | 19.39 | 13.00 | 75.91 | 57.09 | 20.06 | 178.74 | 958.20 | 1290.00 | 1290.00 |
| 6 | 8.48 | 7.56 | 18.14 | 13.00 | 74.77 | 64.00 | 26.16 | 198.96 | 1046.11 | 1410.00 | 1410.00 |
| 7 | 6.70 | 6.58 | 16.57 | 13.00 | 63.93 | 57.26 | 32.29 | 217.44 | 1279.08 | 1650.00 | 1650.00 |
| 8 | 8.80 | 6.40 | 15.56 | 13.00 | 77.15 | 56.29 | 35.62 | 234.21 | 1596.73 | 2000.00 | 2000.00 |
| 9 | 8.73 | 6.64 | 15.65 | 13.00 | 77.27 | 58.66 | 35.22 | 240.04 | 1828.81 | 2240.00 | 2240.00 |
| 10 | 8.55 | 8.17 | 14.86 | 13.00 | 77.15 | 68.95 | 37.60 | 244.57 | 1891.73 | 2320.00 | 2320.00 |
| 11 | 8.27 | 6.79 | 14.24 | 13.01 | 76.73 | 61.30 | 39.47 | 247.74 | 1804.76 | 2230.00 | 2230.00 |
| 12 | 7.28 | 9.56 | 15.18 | 14.20 | 71.02 | 76.98 | 38.60 | 260.58 | 1862.82 | 2310.00 | 2310.00 |
| 13 | 7.12 | 7.06 | 15.30 | 14.91 | 70.81 | 62.75 | 40.42 | 267.78 | 1788.24 | 2230.00 | 2230.00 |
| 14 | 8.34 | 9.90 | 14.75 | 15.04 | 79.92 | 78.72 | 42.38 | 268.80 | 1730.18 | 2200.00 | 2200.00 |
| 15 | 9.16 | 8.72 | 16.44 | 14.05 | 85.24 | 72.64 | 39.92 | 259.81 | 1672.39 | 2130.00 | 2130.00 |
| 16 | 8.78 | 8.18 | 16.32 | 15.30 | 83.24 | 69.40 | 40.67 | 271.20 | 1605.49 | 2070.00 | 2070.00 |
| 17 | 8.50 | 8.16 | 16.32 | 15.23 | 81.67 | 68.68 | 42.48 | 270.66 | 1666.51 | 2130.00 | 2130.00 |
| 18 | 7.80 | 8.49 | 15.05 | 14.74 | 77.11 | 69.20 | 46.78 | 266.25 | 1680.67 | 2140.00 | 2140.00 |
| 19 | 7.28 | 8.47 | 15.25 | 16.42 | 73.39 | 68.24 | 47.26 | 280.80 | 1770.31 | 2240.00 | 2240.00 |
| 20 | 8.39 | 11.03 | 12.75 | 16.92 | 80.43 | 78.98 | 51.11 | 284.24 | 1785.24 | 2280.00 | 2280.00 |
| 21 | 7.22 | 10.81 | 10.00 | 18.05 | 72.48 | 76.89 | 51.34 | 290.98 | 1748.31 | 2240.00 | 2240.00 |
| 22 | 6.49 | 10.89 | 10.00 | 17.99 | 67.22 | 75.97 | 53.23 | 287.69 | 1635.89 | 2120.00 | 2120.00 |
| 23 | 5.99 | 11.72 | 10.02 | 20.57 | 63.48 | 76.60 | 54.96 | 297.96 | 1357.00 | 1850.00 | 1850.00 |
| 24 | 5.41 | 13.42 | 10.09 | 22.13 | 58.80 | 77.74 | 56.22 | 294.46 | 1102.77 | 1590.00 | 1590.00 |

TABLE VIII
THE OPTIMAL SCHEDULING SOLUTION OF CASE 1 IN SYSTEM II

| Time (hour) | Hydro discharge (10^4 m^3) | | | | Hydro generation (MW) | | | | Thermal generation (MW) | | | P_{total} (MW) | P_{load} (MW) |
|----------------|--|----------|----------|----------|-----------------------|----------|----------|----------|-------------------------|----------|----------|----------------------------|---------------------------|
| | Q_{h1} | Q_{h2} | Q_{h3} | Q_{h4} | P_{h1} | P_{h2} | P_{h3} | P_{h4} | P_{t1} | P_{t2} | P_{t3} | | |
| 1 | 6.21 | 6.05 | 18.30 | 6.56 | 63.40 | 50.51 | 48.17 | 135.99 | 102.35 | 209.82 | 139.76 | 750.00 | 750.00 |
| 2 | 5.00 | 6.45 | 29.84 | 6.41 | 53.89 | 54.18 | 0.00 | 130.25 | 102.33 | 209.82 | 229.52 | 780.00 | 780.00 |
| 3 | 11.07 | 7.62 | 17.14 | 7.07 | 92.20 | 62.58 | 42.26 | 133.41 | 20.00 | 209.82 | 139.73 | 700.00 | 700.00 |
| 4 | 9.63 | 7.45 | 29.96 | 7.92 | 84.95 | 62.45 | 0 | 135.58 | 102.35 | 124.91 | 139.76 | 650.00 | 650.00 |
| 5 | 8.79 | 8.58 | 20.19 | 6.60 | 79.58 | 68.86 | 23.20 | 131.11 | 102.58 | 124.91 | 139.76 | 670.00 | 670.00 |
| 6 | 6.27 | 7.24 | 15.68 | 9.19 | 62.99 | 60.62 | 41.86 | 182.29 | 102.66 | 209.82 | 139.76 | 800.00 | 800.00 |
| 7 | 7.08 | 6.45 | 15.90 | 14.75 | 69.24 | 55.12 | 42.63 | 241.07 | 102.60 | 209.82 | 229.52 | 950.00 | 950.00 |
| 8 | 6.86 | 6.84 | 16.62 | 10.49 | 68.16 | 57.86 | 40.91 | 216.17 | 102.66 | 294.72 | 229.52 | 1010.00 | 1010.00 |
| 9 | 10.50 | 6.30 | 10.24 | 15.53 | 89.13 | 55.11 | 47.65 | 271.23 | 102.64 | 294.72 | 229.52 | 1090.00 | 1090.00 |
| 10 | 7.69 | 6.32 | 11.78 | 15.64 | 74.72 | 56.65 | 49.47 | 272.26 | 102.66 | 294.72 | 229.52 | 1080.00 | 1080.00 |
| 11 | 10.95 | 11.38 | 29.94 | 19.60 | 92.48 | 83.21 | 0 | 297.47 | 102.60 | 294.72 | 229.52 | 1100.00 | 1100.00 |
| 12 | 8.57 | 8.07 | 17.23 | 13.14 | 80.93 | 66.68 | 37.00 | 248.73 | 102.66 | 294.72 | 319.28 | 1150.00 | 1150.00 |
| 13 | 6.90 | 9.20 | 13.48 | 19.97 | 70.40 | 72.34 | 47.42 | 292.93 | 102.67 | 294.72 | 229.52 | 1110.00 | 1110.00 |
| 14 | 6.35 | 6.86 | 15.15 | 12.05 | 66.80 | 59.58 | 47.92 | 228.80 | 102.67 | 294.72 | 229.52 | 1030.00 | 1030.00 |
| 15 | 6.55 | 6.73 | 18.31 | 19.32 | 68.81 | 59.87 | 39.36 | 299.95 | 102.67 | 209.82 | 229.52 | 1010.00 | 1010.00 |
| 16 | 6.57 | 7.93 | 28.74 | 19.02 | 69.14 | 67.68 | 0 | 296.27 | 102.67 | 294.72 | 229.52 | 1060.00 | 1060.00 |
| 17 | 12.79 | 7.25 | 13.79 | 19.93 | 103.35 | 63.20 | 46.42 | 295.03 | 102.67 | 209.82 | 229.52 | 1050.00 | 1050.00 |
| 18 | 8.49 | 10.75 | 13.53 | 18.63 | 82.93 | 79.48 | 47.27 | 283.41 | 102.67 | 294.72 | 229.52 | 1120.00 | 1120.00 |
| 19 | 6.37 | 6.13 | 12.41 | 16.71 | 67.27 | 53.52 | 50.69 | 271.61 | 102.67 | 294.72 | 229.52 | 1070.00 | 1070.00 |
| 20 | 9.20 | 11.54 | 11.95 | 17.42 | 86.93 | 81.02 | 51.97 | 288.07 | 102.67 | 209.82 | 229.52 | 1050.00 | 1050.00 |
| 21 | 5.04 | 10.15 | 10.01 | 16.12 | 55.40 | 74.40 | 52.34 | 275.61 | 102.67 | 209.82 | 139.76 | 910.00 | 910.00 |
| 22 | 9.78 | 12.37 | 10.38 | 15.32 | 90.25 | 80.89 | 54.33 | 267.19 | 102.67 | 124.91 | 139.76 | 860.00 | 860.00 |
| 23 | 5.05 | 13.82 | 10.08 | 19.62 | 55.59 | 80.65 | 55.21 | 291.21 | 102.67 | 124.91 | 139.76 | 850.00 | 850.00 |
| 24 | 13.30 | 10.51 | 13.60 | 19.99 | 104.11 | 67.96 | 58.94 | 284.32 | 20.00 | 124.91 | 139.76 | 800.00 | 800.00 |

TABLE IX
THE OPTIMAL SCHEDULING SOLUTION OF CASE 2 IN SYSTEM II

| Time (hour) | Hydro discharge (10^4 m^3) | | | | Hydro generation (MW) | | | | Thermal generation (MW) | | | P_{loss} (MW) | P_{total} (MW) | P_{load} (MW) |
|----------------|--|----------|----------|----------|-----------------------|----------|----------|----------|-------------------------|----------|----------|---------------------------|----------------------------|---------------------------|
| | Q_{h1} | Q_{h2} | Q_{h3} | Q_{h4} | P_{h1} | P_{h2} | P_{h3} | P_{h4} | P_{t1} | P_{t2} | P_{t3} | | | |
| 1 | 11.19 | 7.34 | 30.00 | 7.85 | 90.39 | 58.39 | 0 | 151.10 | 103.17 | 124.91 | 229.52 | 7.74 | 757.74 | 750.00 |
| 2 | 11.80 | 6.84 | 16.20 | 6.96 | 91.21 | 55.83 | 47.79 | 135.64 | 103.42 | 124.91 | 229.52 | 7.31 | 787.31 | 780.00 |
| 3 | 5.26 | 6.22 | 21.36 | 6.21 | 54.52 | 53.19 | 25.64 | 121.41 | 102.65 | 209.82 | 139.76 | 6.99 | 706.99 | 700.00 |
| 4 | 5.71 | 6.52 | 17.67 | 7.55 | 58.57 | 56.63 | 42.86 | 130.54 | 102.58 | 124.91 | 139.76 | 5.84 | 655.84 | 650.00 |
| 5 | 5.60 | 6.06 | 13.56 | 6.25 | 57.70 | 54.43 | 51.33 | 136.99 | 20.00 | 124.86 | 229.52 | 4.83 | 674.83 | 670.00 |
| 6 | 7.92 | 6.34 | 20.23 | 10.31 | 74.49 | 56.78 | 31.67 | 192.10 | 102.60 | 209.82 | 139.76 | 7.20 | 807.20 | 800.00 |
| 7 | 5.13 | 6.22 | 14.22 | 7.61 | 54.09 | 55.83 | 49.68 | 171.42 | 102.64 | 209.82 | 319.28 | 12.75 | 962.75 | 950.00 |
| 8 | 5.46 | 6.04 | 17.32 | 13.71 | 57.65 | 55.00 | 42.79 | 243.58 | 102.59 | 294.72 | 229.52 | 15.85 | 1025.85 | 1010.00 |
| 9 | 5.95 | 6.79 | 15.96 | 11.46 | 62.46 | 60.91 | 45.12 | 222.66 | 102.63 | 294.72 | 319.28 | 17.77 | 1107.77 | 1090.00 |
| 10 | 8.55 | 8.60 | 19.94 | 8.68 | 81.72 | 72.40 | 28.35 | 198.76 | 102.66 | 294.72 | 319.28 | 17.89 | 1097.89 | 1080.00 |
| 11 | 10.70 | 7.08 | 16.37 | 17.31 | 93.44 | 64.01 | 40.12 | 284.13 | 102.56 | 209.82 | 319.28 | 13.35 | 1113.35 | 1100.00 |
| 12 | 9.80 | 6.65 | 15.28 | 13.79 | 89.19 | 61.70 | 43.43 | 256.98 | 102.66 | 294.72 | 319.28 | 17.96 | 1167.96 | 1150.00 |
| 13 | 9.25 | 9.51 | 16.36 | 16.90 | 86.55 | 78.33 | 43.57 | 283.50 | 102.29 | 209.82 | 319.28 | 13.34 | 1123.34 | 1110.00 |
| 14 | 9.06 | 8.61 | 18.08 | 18.92 | 86.01 | 73.58 | 39.06 | 299.00 | 102.64 | 209.82 | 229.52 | 9.63 | 1039.63 | 1030.00 |
| 15 | 6.71 | 6.36 | 13.98 | 19.03 | 70.08 | 60.38 | 50.02 | 297.05 | 102.63 | 209.82 | 229.52 | 9.49 | 1019.49 | 1010.00 |
| 16 | 10.16 | 10.35 | 23.02 | 13.46 | 92.87 | 82.87 | 15.45 | 253.06 | 104.71 | 294.72 | 229.52 | 13.20 | 1073.20 | 1060.00 |
| 17 | 12.07 | 9.95 | 14.75 | 17.78 | 100.39 | 79.31 | 49.12 | 288.93 | 102.55 | 209.82 | 229.52 | 9.63 | 1059.63 | 1050.00 |
| 18 | 7.90 | 10.04 | 16.30 | 19.43 | 78.74 | 77.43 | 46.90 | 298.59 | 102.64 | 209.82 | 319.28 | 13.40 | 1133.40 | 1120.00 |
| 19 | 9.33 | 7.19 | 10.02 | 13.64 | 87.38 | 61.27 | 52.85 | 252.77 | 104.48 | 294.72 | 229.52 | 12.99 | 1082.99 | 1070.00 |
| 20 | 7.30 | 11.65 | 13.63 | 20.00 | 73.95 | 81.93 | 56.04 | 305.51 | 102.87 | 209.82 | 229.52 | 9.64 | 1059.64 | 1050.00 |
| 21 | 5.07 | 9.48 | 12.13 | 16.56 | 55.54 | 72.06 | 57.97 | 279.85 | 102.67 | 209.82 | 139.76 | 7.66 | 917.66 | 910.00 |
| 22 | 5.30 | 12.55 | 12.28 | 18.79 | 57.85 | 82.37 | 58.82 | 293.60 | 20.00 | 124.91 | 229.52 | 7.07 | 867.07 | 860.00 |
| 23 | 8.39 | 11.84 | 19.80 | 12.87 | 82.22 | 77.30 | 45.12 | 284.85 | 102.67 | 124.91 | 139.76 | 6.82 | 856.82 | 850.00 |
| 24 | 11.40 | 12.76 | 12.87 | 19.99 | 97.97 | 78.57 | 58.98 | 284.35 | 20.00 | 124.63 | 139.76 | 4.27 | 804.27 | 800.00 |

TABEL X
THE OPTIMAL SCHEDULING SOLUTION OF HYDRO PLANTS IN SYSTEM III

| Time (hour) | Hydro discharge (10^4 m^3) | | | | Hydro generation (MW) | | | | Total hydro generation (MW) |
|----------------|--|----------|----------|----------|-----------------------|----------|----------|----------|--------------------------------|
| | Q_{h1} | Q_{h2} | Q_{h3} | Q_{h4} | P_{h1} | P_{h2} | P_{h3} | P_{h4} | |
| 1 | 7.34 | 7.14 | 17.53 | 5.14 | 71.50 | 57.22 | 50.69 | 118.05 | 297.46 |
| 2 | 9.27 | 5.30 | 28.44 | 7.02 | 83.19 | 45.89 | 0.00 | 138.86 | 267.94 |
| 3 | 8.14 | 6.00 | 17.15 | 7.05 | 76.64 | 52.70 | 43.42 | 133.98 | 306.74 |
| 4 | 11.71 | 4.43 | 22.58 | 4.70 | 91.60 | 42.94 | 16.93 | 98.38 | 249.85 |
| 5 | 5.96 | 8.54 | 14.33 | -8.69 | 59.93 | 71.32 | 48.55 | 0.00 | 179.81 |
| 6 | 9.80 | 6.10 | 14.47 | 17.13 | 83.10 | 55.94 | 50.67 | 266.84 | 456.55 |
| 7 | 7.98 | 7.58 | 21.67 | 10.56 | 73.33 | 65.18 | 22.83 | 212.01 | 373.35 |
| 8 | 9.09 | 11.74 | 14.66 | 12.15 | 79.60 | 83.27 | 49.61 | 238.39 | 450.87 |
| 9 | 5.80 | 6.61 | 21.03 | 16.89 | 58.98 | 57.00 | 26.17 | 279.77 | 421.93 |
| 10 | 8.91 | 8.67 | 13.02 | 17.81 | 80.81 | 69.97 | 50.68 | 283.20 | 484.67 |
| 11 | 5.93 | 7.88 | 25.26 | 20.50 | 61.78 | 65.95 | 0.00 | 301.19 | 428.93 |
| 12 | 7.30 | 8.09 | 14.92 | 15.63 | 72.87 | 67.21 | 47.46 | 266.56 | 454.10 |
| 13 | 12.30 | 9.81 | 19.60 | 19.29 | 97.69 | 75.51 | 32.95 | 295.02 | 501.17 |
| 14 | 6.74 | 10.04 | 15.24 | 15.78 | 69.34 | 75.96 | 47.57 | 266.85 | 459.72 |
| 15 | 9.22 | 10.30 | 10.88 | 17.11 | 86.35 | 76.39 | 52.79 | 285.27 | 500.79 |
| 16 | 7.44 | 8.46 | 19.88 | 16.51 | 75.25 | 66.68 | 37.17 | 279.07 | 458.17 |
| 17 | 9.49 | 6.84 | 9.65 | 18.06 | 88.30 | 56.78 | 53.15 | 292.21 | 490.43 |
| 18 | 7.57 | 12.19 | 9.84 | 17.33 | 76.14 | 79.55 | 55.19 | 284.91 | 495.79 |
| 19 | 6.59 | 9.88 | 20.67 | 20.10 | 68.79 | 68.25 | 40.31 | 293.39 | 470.74 |
| 20 | 8.66 | 5.39 | 9.84 | 16.39 | 83.08 | 42.79 | 55.77 | 272.10 | 453.74 |
| 21 | 6.80 | 8.41 | 15.47 | 15.89 | 70.14 | 62.82 | 58.54 | 261.89 | 453.38 |
| 22 | 5.90 | 10.13 | 15.46 | 13.33 | 62.96 | 70.83 | 59.55 | 235.95 | 429.30 |
| 23 | 8.69 | 10.86 | 18.40 | 16.83 | 83.72 | 72.02 | 52.03 | 269.57 | 477.34 |
| 24 | 8.39 | 11.61 | 19.63 | 14.97 | 82.05 | 72.26 | 46.36 | 249.49 | 450.16 |

TABEL XI
THE OPTIMAL SCHEDULING SOLUTION OF THERMAL PLANTS IN SYSTEM III

| Time (hour) | Thermal generation (MW) | | | | | | | | | | P_{thermal} (MW) | P_{total} (MW) | P_{load} (MW) |
|----------------|-------------------------|----------|----------|----------|----------|----------|----------|----------|----------|-----------|------------------------------|----------------------------|---------------------------|
| | P_{t1} | P_{t2} | P_{t3} | P_{t4} | P_{t5} | P_{t6} | P_{t7} | P_{t8} | P_{t9} | P_{t10} | | | |
| 1 | 319.28 | 199.60 | 94.80 | 119.73 | 224.47 | 139.73 | 45.00 | 35.00 | 98.06 | 176.87 | 1452.54 | 1750.00 | 1750.00 |
| 2 | 319.28 | 199.60 | 94.80 | 119.73 | 224.47 | 139.73 | 104.28 | 35.00 | 98.06 | 177.12 | 1512.06 | 1780.00 | 1780.00 |
| 3 | 319.28 | 199.60 | 20.31 | 119.73 | 174.60 | 139.73 | 45.00 | 35.00 | 160.00 | 180.00 | 1393.26 | 1700.00 | 1700.00 |
| 4 | 229.52 | 274.40 | 94.80 | 119.73 | 124.73 | 139.73 | 104.28 | 35.00 | 98.06 | 179.90 | 1400.15 | 1650.00 | 1650.00 |
| 5 | 319.28 | 274.40 | 94.80 | 119.73 | 124.73 | 139.73 | 104.28 | 35.00 | 98.24 | 180.00 | 1490.19 | 1670.00 | 1670.00 |
| 6 | 319.28 | 199.60 | 20.38 | 119.73 | 124.73 | 139.73 | 45.00 | 35.00 | 160.00 | 180.00 | 1343.45 | 1800.00 | 1800.00 |
| 7 | 409.04 | 274.40 | 94.80 | 119.73 | 124.73 | 139.73 | 104.28 | 35.00 | 98.06 | 176.87 | 1576.65 | 1950.00 | 1950.00 |
| 8 | 229.52 | 274.40 | 94.80 | 119.73 | 224.47 | 139.73 | 104.28 | 35.00 | 160.00 | 177.20 | 1559.13 | 2010.00 | 2010.00 |
| 9 | 229.52 | 274.40 | 94.80 | 119.73 | 224.47 | 189.60 | 163.55 | 35.00 | 160.00 | 177.01 | 1668.07 | 2090.00 | 2090.00 |
| 10 | 319.28 | 274.40 | 94.80 | 119.73 | 224.47 | 139.73 | 163.55 | 35.00 | 98.06 | 126.31 | 1595.33 | 2080.00 | 2080.00 |
| 11 | 319.28 | 349.20 | 94.80 | 119.73 | 174.60 | 139.73 | 163.55 | 35.00 | 98.06 | 177.12 | 1671.07 | 2100.00 | 2100.00 |
| 12 | 319.28 | 274.40 | 94.80 | 119.73 | 224.47 | 189.60 | 163.55 | 35.00 | 98.06 | 177.01 | 1695.90 | 2150.00 | 2150.00 |
| 13 | 229.52 | 274.40 | 94.80 | 119.73 | 224.47 | 189.60 | 104.28 | 35.00 | 160.00 | 177.04 | 1608.83 | 2110.00 | 2110.00 |
| 14 | 409.04 | 274.40 | 94.80 | 119.73 | 174.60 | 139.73 | 45.00 | 35.00 | 98.06 | 179.91 | 1570.28 | 2030.00 | 2030.00 |
| 15 | 229.52 | 274.40 | 94.80 | 119.73 | 174.60 | 139.73 | 104.28 | 35.00 | 160.00 | 177.15 | 1509.21 | 2010.00 | 2010.00 |
| 16 | 319.28 | 274.40 | 94.81 | 119.73 | 174.60 | 139.73 | 104.28 | 35.00 | 160.00 | 180.00 | 1601.83 | 2060.00 | 2060.00 |
| 17 | 229.52 | 274.40 | 94.80 | 119.73 | 224.47 | 139.73 | 163.55 | 35.00 | 98.36 | 180.00 | 1559.57 | 2050.00 | 2050.00 |
| 18 | 229.52 | 349.20 | 94.80 | 119.73 | 224.47 | 189.60 | 45.00 | 35.00 | 160.00 | 176.89 | 1624.21 | 2120.00 | 2120.00 |
| 19 | 319.28 | 274.40 | 94.80 | 119.73 | 174.60 | 139.73 | 163.55 | 35.00 | 98.16 | 180.00 | 1599.26 | 2070.00 | 2070.00 |
| 20 | 319.28 | 274.40 | 94.80 | 119.73 | 174.60 | 139.73 | 163.55 | 35.00 | 98.06 | 177.11 | 1596.26 | 2050.00 | 2050.00 |
| 21 | 229.52 | 274.40 | 94.80 | 119.73 | 124.73 | 139.73 | 163.55 | 35.00 | 98.06 | 177.09 | 1456.62 | 1910.00 | 1910.00 |
| 22 | 319.28 | 274.40 | 94.80 | 119.73 | 124.73 | 139.73 | 45.00 | 35.00 | 98.06 | 179.96 | 1430.70 | 1860.00 | 1860.00 |
| 23 | 229.52 | 199.60 | 94.80 | 119.73 | 174.60 | 139.73 | 104.28 | 35.00 | 98.06 | 177.34 | 1372.66 | 1850.00 | 1850.00 |
| 24 | 229.52 | 274.40 | 94.80 | 119.73 | 124.73 | 139.73 | 45.00 | 35.00 | 160.00 | 126.92 | 1349.84 | 1800.00 | 1800.00 |

REFERENCES

- [1] G. Chen, M. Gao, Z. Zhang and S. Li, "Hybridization of Chaotic Grey Wolf Optimizer and Dragonfly Algorithm for Short-term Hydrothermal Scheduling," *IEEE Access*, vol. 8, pp142996-143020, 2020.
- [2] G. Cavazzini, G. Pavesi and G. Ardizzone, "A Novel Two-swarm Based PSO Search Strategy for Optimal Short-term Hydro-thermal Generation Scheduling," *Energy Conversion and Management*, vol. 164, pp460-481, 2018.
- [3] G. Chen, Y. Xiao, F. Long, X. Hu and H. Long, "An Improved Marine Predators Algorithm for Short-term Hydrothermal Scheduling," *IAENG International Journal of Applied Mathematics*, vol. 51, no. 1, pp936-949, 2021.
- [4] J. Jian, S. Pan and L. Yang, "Solution for Short-term Hydrothermal Scheduling with A Logarithmic Size Mixed-integer Linear Programming Formulation," *Energy*, vol. 177, pp770-784, 2019.
- [5] X. Guan, P. B. Luh and L. Zhang, "Nonlinear Approximation Method in Lagrangian Relaxation-based Algorithms for Hydrothermal Scheduling," *IEEE Transactions on Power Systems*, vol. 10, pp772-778, 1995.
- [6] S. Chang, C. Chen, I. Fong and P. B. Luh, "Hydroelectric Generation Scheduling with An Effective Differential Dynamic Programming Algorithm," *IEEE Transactions on Power Systems*, vol. 5, pp737-743, 1990.
- [7] G. W. Chang, M. Aganagic, J. G. Waight and J. Medina, et al., "Experiences with Mixed Integer Linear Programming Based Approaches on Short-term Hydro Scheduling," *IEEE Transactions on Power Systems*, vol. 16, pp743-749, 2001.
- [8] M. S. Salam, K. M. Nor and A. R. Hamdan, "Hydrothermal Scheduling Based Lagrangian Relaxation Approach to Hydrothermal Coordination," *IEEE Transactions on Power Systems*, vol. 13, pp226-235, 1998.
- [9] H. Zhang, D. Yue and X. Xie, "Gradient Decent Based Multi-objective Cultural Differential Evolution for Short-term Hydrothermal Optimal Scheduling of Economic Emission with Integrating Wind Power and Photovoltaic Power," *Energy*, vol. 122, pp748-776, 2017.
- [10] M. F. Zaghlool and F. C. Trutt, "Efficient Methods for Optimal Scheduling of Fixed Head Hydrothermal Power Systems," *IEEE Transactions on Power Systems*, vol. 3, pp24-30, 1988.
- [11] V. S. Kumar and M. R. Mohan, "A Genetic Algorithm Solution to the Optimal Short-term Hydrothermal Scheduling," *International Journal of Electrical Power & Energy Systems*, vol. 33, pp827-835, 2011.
- [12] K. K. Mandal and N. Chakraborty, "Short-term Combined Economic Emission Scheduling of Hydrothermal Power Systems with Cascaded Reservoirs Using Differential Evolution," *Energy Conversion and Management*, vol. 50, pp97-104, 2009.
- [13] B. Yu, X. Yuan and J. Wang, "Short-term Hydro-thermal Scheduling Using Particle Swarm Optimization Method," *Energy Conversion and Management*, vol. 48, pp1902-1908, 2007.
- [14] M. Basu, "Hopfield Neural Networks for Optimal Scheduling of Fixed Head Hydrothermal Power Systems," *Electric Power Systems Research*, vol. 64, pp11-15, 2003.
- [15] Tehzeeb-ul-Hassan, T. Alquthami, S. E. Butt, M. F. Tahir and K. Mehmood, "Short-term Optimal Scheduling of Hydro-thermal Power Plants Using Artificial Bee Colony Algorithm," *Energy Reports*, vol. 6, pp984-992, 2020.
- [16] X. Zeng, A. T. Hammid, N. M. Kumar, U. Subramaniam and D. J. Almakhlis, "A Grasshopper Optimization Algorithm for Optimal Short-term Hydrothermal Scheduling," *Energy Reports*, vol. 7, pp314-323, 2021.
- [17] J. Zhang, S. Lin and W. Qiu, "A Modified Chaotic Differential Evolution Algorithm for Short-term Optimal Hydrothermal Scheduling," *International Journal of Electrical Power & Energy Systems*, vol. 65, pp159-168, 2015.
- [18] J. Sasikala and M. Ramaswamy, "Optimal Gamma Based Fixed Head Hydrothermal Scheduling Using Genetic Algorithm," *Expert Systems with Applications*, vol. 37, pp3352-3357, 2010.
- [19] T. T. Nguyen and D. N. Vo, "Modified Cuckoo Search Algorithm for Short-term Hydrothermal Scheduling," *International Journal of Electrical Power & Energy Systems*, vol. 65, pp271-281, 2015.
- [20] A. Naik, S. C. Satapathy and A. Abraham, "Modified Social Group Optimization—A Meta-heuristic Algorithm to Solve Short-term Hydrothermal Scheduling," *Applied Soft Computing*, vol. 95, pp106524, 2020.
- [21] M. S. Fakhar, S. A. R. Kashif, S. Liaquat and A. Rasool, et al., "Implementation of APSO and Amproved APSO on Non-cascaded and Cascaded Short Term Hydrothermal Hcheduling," *IEEE Access*, vol. 9, pp77784-77797, 2021.
- [22] N. Fang, J. Zhou, R. Zhang, Y. Liu and Y. Zhang, "A Hybrid of Real Coded Genetic Algorithm and Artificial Fish Swarm Algorithm for Short-term Optimal Hydrothermal Scheduling," *International Journal of Electrical Power & Energy Systems*, vol. 62, pp617-629, 2014.
- [23] M. Khishe and M. R. Mosavi, "Chimp Optimization Algorithm," *Expert Systems with Applications*, vol. 149, pp113338, 2020.
- [24] S. Mirjalili and A. Lewis, "The Whale Optimization Olgorithm," *Advances in Engineering Software*, vol. 95, pp51-67, 2016.
- [25] S. Mirjalili, S. M. Mirjalili and A. Lewis, "Grey Wolf Optimizer," *Advances in Engineering Software*, vol. 69, pp46-61, 2014.
- [26] J. Zhang and J. S. Wang, "Improved Whale Optimization Algorithm Based on Nonlinear Adaptive Weight and Golden Sine Operator," *IEEE Access*, vol. 8, pp77013-77048, 2020.
- [27] M. W. Guo, J. S. Wang, L. F. Zhu, S. S. Guo and W. Xie, "An Improved Grey Wolf Optimizer Based on Tracking and Seeking Modes to Solve Function Optimization Problems," *IEEE Access*, vol. 8, pp69861-69893, 2020.
- [28] K. K. Mandal, M. Basu and N. Chakraborty, "Particle Swarm Optimization Technique Based Short-term Hydrothermal Scheduling," *Applied Soft Computing*, vol. 8, pp1392-1399, 2008.
- [29] E. Rashedi, H. Nezamabadi-pour and S. Saryazdi, "GSA: A Gravitational Search Algorithm," *Information Sciences*, vol. 179, pp2232-2248, 2009.
- [30] X. Yuan, B. Ji, Z. Chen and Z. Chen, "A Novel Approach for Economic Dispatch of Hydrothermal System Via Gravitational Search Algorithm," *Applied Mathematics and Computation*, vol. 247, pp535-546, 2014.
- [31] O. Hoseynpour, B. Mohammadi-ivatloo, M. Nazari-Heris and S. Asadi, "Application of Dynamic Non-Linear Programming Technique to Non-convex Short-term Hydrothermal Scheduling Problem," *Energies*, vol. 10, pp1440, 2017.
- [32] P. K. Roy, C. Paul and S. Sultana, "Oppositional Teaching Learning Based Optimization Approach for Combined Heat and Power Dispatch," *International Journal of Electrical Power & Energy Systems*, vol. 57, pp392-403, 2014.
- [33] H. E. Qing, L. Jie and X. U. Hang, "Hybrid Cauchy Mutation and Uniform Distribution of Grasshopper Optimization Algorithm," *Control and Decision*, vol. 36, pp1558-1568, 2021.
- [34] S. O. Orero and M. R. Irving, "A Genetic Algorithm Modelling Framework and Solution Technique for Short Term Optimal Hydrothermal Scheduling," *IEEE Transactions on Power Systems*, vol. 13, pp501-518, 1998.
- [35] Y. Wang, J. Zhou, L. Mo, R. Zhang and Y. Zhang, "Short-term Hydrothermal Generation Scheduling Using Differential Real-coded Quantum-inspired Evolutionary Algorithm," *Energy*, vol. 44, pp657-671, 2012.
- [36] J. Zhang, S. Lin, H. Liu and Y. Chen, et al., "A Small-population Based Parallel Differential Evolution Algorithm for Short-term Hydrothermal Scheduling Problem Considering Power Flow Constraints," *Energy*, vol. 123, pp538-554, 2017.
- [37] L. Lakshminarasimman and S. Subramanian, "Short-term Scheduling of Hydrothermal Power System with Cascaded Reservoirs by Using Modified Differential Evolution," *IEE Proceedings - Generation, Transmission and Distribution*, vol. 153, pp693-700, 2006.
- [38] H. M. Dubey, M. Pandit and B. K. Panigrahi, "Ant Lion Optimization for Short-term Wind Integrated Hydrothermal Power Generation Scheduling," *International Journal of Electrical Power & Energy Systems*, vol. 83, pp158-174, 2016.
- [39] H. Omid, M. Behnam, N. Morteza and A. Somayeh, "Application of Dynamic Non-Linear Programming Technique to Non-convex Short-term Hydrothermal Scheduling problem," *Energies*, vol. 10, pp1440-1457, 2017.
- [40] K. Bhattacharjee, A. Bhattacharya and S. Halder Nee Dey, "Oppositional Real Coded Chemical Reaction Based Optimization to Solve Short-term Hydrothermal Scheduling Problems," *International Journal of Electrical Power & Energy Systems*, vol. 63, pp145-157, 2014.
- [41] N. Gouthamkumar, V. Sharma and R. Naresh, "Disruption Based Gravitational Search Algorithm for Short Term Hydrothermal Scheduling," *Expert Systems with Applications*, vol. 42, pp7000-7011, 2015.
- [42] P. K. Roy, A. Sur and D. K. Pradhan, "Optimal Short-term Hydro-thermal Scheduling Using Quasi-oppositional Teaching Learning Based Optimization," *Engineering Applications of Artificial Intelligence*, vol. 26, pp2516-2524, 2013.

- [43] A. Rasoulzadeh-Akhijahani and B. Mohammadi-Ivatloo, "Short-term Hydrothermal Generation Scheduling by A Modified Dynamic Neighborhood Learning Based Particle Swarm Optimization," *International Journal of Electrical Power & Energy Systems*, vol. 67, pp350-367, 2015.
- [44] M. Basu, "Quasi-oppositional Group Search Optimization for Hydrothermal Power System," *International Journal of Electrical Power & Energy Systems*, vol. 81, pp324-335, 2016.
- [45] S. Das and A. Bhattacharya, "Symbiotic Organisms Search Algorithm for Short-term Hydrothermal Scheduling," *Ain Shams Engineering Journal*, vol. 9, pp499-516, 2016.
- [46] J. Zhang, J. Wang and C. Yue, "Small Population-based Particle Swarm Optimization for Short-term Hydrothermal Scheduling," *IEEE Transactions on Power Systems*, vol. 27, pp142-152, 2012.